NATIONAL ENERGY TECHNOLOGY LABORATORY

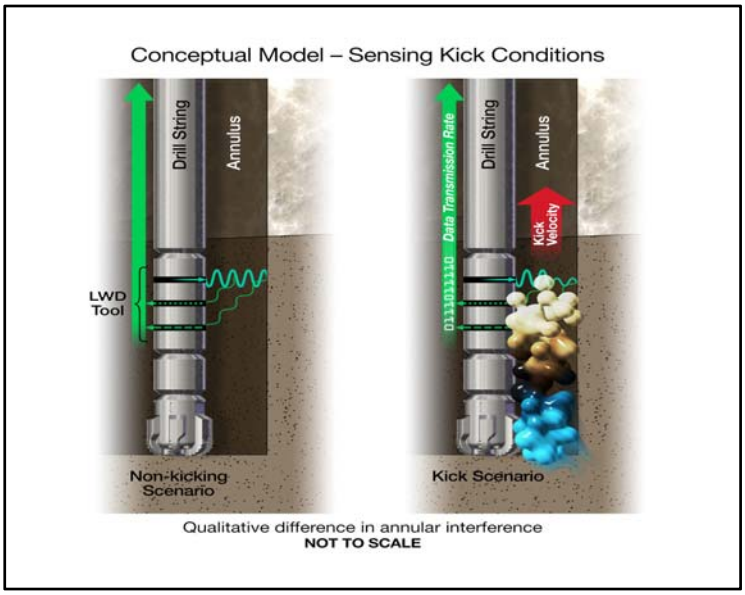

Kick Detection at the Bit: Early Detection via Low Cost Monitoring

7 June 2016

U.S. DEPARTMENT OF ENERGY

Office of Fossil Energy

NETL-TRS-2-2016

Disclaimer

Cover Illustration: A conceptual model contrasting the signal medium responses by geophysical instrumentation in kicking and non-kicking wellbores.

Suggested Citation: Tost, B.; Rose, K.; Aminzadeh, F.; Ante, M. A.; Huerta, N. *Kick Detection at the Bit: Early Detection via Low Cost Monitoring*; NETL-TRS-2-2016; EPAct Technical Report Series; U.S. Department of Energy, National Energy Technology Laboratory: Albany, OR, 2016; p. 48.

An electronic version of this report can be found at:
http://www.netl.doe.gov/research/on-site-research/publications/featured-technical-reports

https://edx.netl.doe.gov/offshore

Kick Detection at the Bit: Early Detection via Low Cost Monitoring

Brian Tost[1], Kelly Rose[2], Fred Aminzadeh[3], Magdalene A. Ante[3], Nicolas Huerta[2]

[1] Oak Ridge Institute for Science and Education (ORISE), U.S. Department of Energy, National Energy Technology Laboratory, 1450 Queen Avenue SW, Albany, OR 97321

[2] U.S. Department of Energy, National Energy Technology Laboratory, 1450 Queen Avenue SW, Albany, OR 97321

[3] Department of Petroleum Engineering, University of Southern California, 925 Bloom Walk, HED 309, Los Angeles, CA 90089

NETL-TRS-2-2016

7 June 2016

NETL Contacts:

Kelly Rose, Principal Investigator

Kelly Rose, Technical Coordinator

Cynthia Powell, Executive Director, Research and Innovation Center

This page intentionally left blank.

Table of Contents

List of Figures

List of Tables

Acronyms, Abbreviations, and Symbols

Term	Description
ANN	Artificial neural network
API	American Petroleum Institute
DWT	Discrete wavelet transforms
EKLD	Early Kick/Loss Detection
EM	Electromagnetic
e.m.f.	Electromotive force
LWD	Logging while drilling
MWD	Measurement while drilling
OBM	Oil-based drilling fluid (mud)
ROP	Rate-of-penetration
WBM	Water-based drilling fluid (mud)

Acknowledgments

This work was completed as part of National Energy Technology Laboratory (NETL) research for the U.S. Department of Energy's (DOE) Complementary Research Program under Section 999 of the Energy Policy Act of 2005. The authors wish to acknowledge Roy Long (NETL Science and Technology Strategic Plans and Programs) and Elena Melchert (DOE Office of Fossil Energy) for programmatic guidance, direction, and support.

ABSTRACT

Formation fluid influxes (i.e. kicks) pose persistent challenges and operational costs during drilling operations. Implications of kicks range in scale but cumulatively result in substantial costs that affect drilling safety, environment, schedule, and infrastructure. Early kick detection presents a low-cost, easily adopted solution for avoiding well control challenges associated with kicks near the bit. Borehole geophysical tools used during the drilling process as part of the logging-while-drilling (LWD) and measurement-while-drilling (MWD) provide the advantage of offering real-time downhole data. LWD/MWD collect data on both the annulus and borehole wall. The annular data are normally treated as background, and are filtered out to isolate the formation measurements. Because kicks will change the local physical properties of annular fluids, bottom-hole measurements are among the first indicators that a formation fluid has invaded the wellbore. This report describes and validates a technique for using the annular portion of LWD/MWD data to facilitate early kick detection using first order principles. The detection technique leverages data from standard and cost-effective technologies that are typically implemented during well drilling, such as MWD/LWD data in combination with mud-pulse telemetry for data transmission.

1. BACKGROUND AND INTRODUCTION

Formation fluid influxes, also referred to as "kicks", can negatively affect wellbore stability on a wide range of scales. Kicks can cause deleterious impacts to safety, the environment, and drilling schedules, and result in substantial costs to operators each year (Halliburton, 2016). A low-cost, easily-implemented kick detection method is required to reduce operational costs and environmental impacts, and improve safety during drilling operations.

The development of while-drilling technology not only represents a critical advancement in the measurement and visualization of the subsurface, but also affords an opportunity to support early, real-time kick detection near the drill bit. Advances in while-drilling technologies have been particularly useful for well control: helping to define safe drilling margins and prevent loss-of-control events. Conventional well logging measurements—generally referred to as wireline measurements—focus on the near-wellbore-formation and are tailored to formation evaluation purposes with corrections made to filter out the effect of materials in the annulus. Logging-while-drilling (LWD) or measurement-while-drilling (MWD) tool suites incorporate similar geophysical instrumentation onto the drillstring to make measurements during the drilling process. The primary advantage of while-drilling measurements over wireline measurements is offering "real-time" information about the formation and fluid properties near the drill bit.

This work presents the theoretical background on a novel method for using while-drilling measurement data to support early kick detection.

1.1 WHILE-DRILLING MEASUREMENTS

Logging-while-drilling generally refers to the measurement of formation rock and fluid properties, such as electrical resistivity, density/porosity, acoustic/sonic velocity, and gamma ray emission. Borehole diameter measured by the caliper log, a potential indicator of formation consolidation/unconsolidation, is also usually included as part of the LWD tool suite.

MWD describes instrumentation that collects data related to drilling mechanics, such as rate-of-penetration and weight-on-bit, and bit steering. MWD modules also typically house the data telemetry capability for the drillstring. In both LWD and MWD, the tools are incorporated into the drillstring in discrete modules referred to as "subs".

This study focuses on while-drilling instruments whose tool configurations (measurement and data) are affected by borehole fluid. Specifically, these are the instruments that measure density, velocity, and electrical resistivity.

1.1.1 Instrumentation Background

Density Instrumentation: Formation density is indirectly measured using the gamma density method. The gamma density method uses a gamma ray source and two detectors (one short-spaced and one long-spaced). The measurement principle is that gamma rays experience Compton scattering when they interact with electrons in elements. Compton scattering is the deflection of both the gamma ray and the electron because of their collision. For the majority of geologically-relevant elements, the amount of Compton scattering is proportional to the atomic mass and, hence, the bulk density (Ellis and Singer, 2007).

To make the gamma density measurement, gamma rays are emitted radially from the tool in the borehole in the direction of the borehole wall. A minority portion of the emitted gamma rays are

back-scattered by the materials in the annulus (e.g. drilling and formation fluids, or formation cuttings). The short-spacing detector receives the annular back-scatter, which is used to correct the long-spacing detector for any annular interference. The gamma rays that reach the borehole wall either pass through the borehole wall or are back-scattered by the formation materials composing the borehole wall.

The gamma ray fraction that is back-scattered by the borehole wall is received by the long-spacing detector, and is used to estimate the formation bulk density. Bulk density measurements are an indicator of lithology change, they provide an estimation of formation porosity (i.e. density porosity), and assist in identifying both the identity and the degree of saturation of pore-filling material in a formation (e.g., gas vs. liquid).

Electrical Resistivity Instrumentation: Formation electrical resistivity may be measured directly or indirectly. Direct resistivity measurements may be made by tools with physical contact with the borehole wall, such as electrode or button resistivity tools. Electrode resistivity measurements are made by placing an electric current source in direct contact with the borehole wall. Electric current is emitted into the formation. The resulting voltage between points on the borehole wall is related to the electrical resistivity. Multiple detectors may be used in electrode resistivity measurements to provide a deeper lateral depth-of-investigation, and a gradient of the electrical resistivity as a function of lateral extent into the formation. Indirect measurement techniques use electromagnetic induction to measure the formation conductivity, which is inverted to determine the formation resistivity. Electromagnetic waves induce electric currents within the formation. The induced currents are then related to the electrical conductivity, which is inverted to determine the electrical resistivity. Electrical resistivity measurements have many applications, such as determining the extent of drilling mud filtrate infiltration into the formation (i.e. the invaded zone), estimating the formation porosity, and providing essential data to assist in identifying formation fluids.

Acoustic Velocity Instrumentation: Borehole sonic/acoustic measurements are based on the principles of wave propagation in elastic media. The source emits an acoustic wave that propagates through the borehole and formation, which returns to the receivers. The waveform is recorded as a function of time, and contains different energy modes dependent on frequency, velocity, and amplitude. The waveform modes of interest for borehole logging are: compressional, shear, and Stoneley waves. Acoustic/sonic velocity measurements are used to estimate the formation porosity, and assist in identifying the type of pore-filling material in a formation (e.g., gas vs. liquid).

1.2 CAUSES OF KICK

The driving force for a kick is the development of a gradient in potential between the geological formation and the fluid-filled borehole. During normal drilling operations (i.e. overbalanced drilling) the drilling fluid is expected to exert pressure in excess of the formations fluid's pore pressure. Drilling fluid densities are formulated according to the margin bounded by the expected formation pore pressure and the expected formation fracture strength. Accurately predicting formation pore pressures in all instances is non-trivial. Overpressured zones, defined as zones where pore pressure is greater than hydrostatic (Osborne and Swarbrick, 1997; van Ruth et al., 2004; Guo et al., 2010), may occur in formations because of disequilibrium compaction (also known as undercompaction), a condition where a sediment is buried faster than its pore fluid can drain, causing abnormally-high pore pressure to build (Swarbrick, 1994), porosity reduction from

mineral transformations in porespace (Swarbrick, 1994), or formation fluid volume changes because of mechanisms such as aquathermal pressuring (Osborne and Swarbrick, 1997; Guo et al., 2010) and fluid diagenesis (Swarbrick, 1994; Osborne and Swarbrick, 1997; Guo et al., 2010). Because it is difficult to account for the variety of causes that could induce an overpressure zone, it is possible for the driller to underestimate formation pore pressures, resulting in a drilling fluid density that is too low to restrain the formation pore pressure, resulting in a pressure gradient from the formation to the borehole.

Drilling fluid density can also be reduced because of use. The weighting materials in drilling fluid can fall out of solution, a condition known as "sag" (Bern et al., 1996). The loss of weighting materials results in a reduction of the drilling fluid density, and hence, a reduction in the hydrostatic pressure that can be developed by the drilling fluid. The loss of pressure by the drilling fluid can result in a pressure gradient developing from the formation in the direction of the borehole, which can result in a kick (Saasen et al., 2002; Choe et al., 2004). Formation fluids in the porespace at the borehole wall can diffuse into the drilling fluid by molecular action, regardless of the pressure regime that exists between the borehole and formation. These formation fluids tend to be lower density than the drilling fluid, which dilutes the drilling fluid and reduces its density. This drilling fluid density reduction because of formation fluid dissolution is also known as "cut" and is usually specified by the contaminant (e.g. "gas-cut", "water-cut", "oil-cut" depending on the formation fluid dissolving into the drilling fluid).

Kicks can also occur because of typical drilling activities. Removal of the drillstring can create a low pressure condition in the borehole which will draw formation fluid into the borehole, a condition referred to as "swabbing" (Choe et al., 2004).

1.3 EXISTING KICK DETECTION TECHNIQUES

Mud logging is the most common and basic method of kick detection. It relies on drilling fluid returns to the rig floor or mud pit to identify when a well being drilled for hydrocarbon or other subsurface purposes is taking on a kick of hydrocarbon, gas, or water from the surrounding formation. With increasing drilling depths in ultra-deep waters, the risk of a blowout due to late kick detection also increases. Bottoms-up circulation for deep wells can be as much as 4 hrs. While waiting for indications that a kick may be occurring (e.g., kick-fluid-cut drilling fluid returns to the rig floor or mud pit), the kick's volume and intensity grows in the borehole. Thus, the time spent waiting for kick indicators reduces the driller's ability to mitigate the potential impacts of a kick; putting life, materials, and the surrounding environment at risk. Additionally, pit gain indicators vary according to kick fluid solubility in a particular drilling mud type. If a gas influx is highly soluble in a drilling mud, a small increase in gains could result from a large influx volume.

Ali et al. (2013) provide a method of kick detection using an automated process to monitor wellbore flowback. The smart system of flowback fingerprinting enables more accurate identification of wellbore breathing and flowback due to static conditions as distinguished from formation fluid influx. Flowback fingerprinting is an analytical process employed during static conditions in which the rates-of-change for multiple successive drilling fluid flowback cycles to the mud pits are compared and analyzed (Baker Hughes, 2014). Under static conditions, drilling fluid flowback cycles have a repeatable profile when measured over successive cycles. Thus, departures from the expected flowback rate-of-change could indicate a formation fluid influx (Baker Hughes, 2014).

Speers et al. (1987) discuss a delta flow approach which uses the output flow rate of the mud system. Magnetic flowmeters designed for water-based mud systems are installed in the pump output line and in the return flowline to detect abnormal well condition. Pore pressure prediction techniques uses LWD and MWD measurements in real time to predict pore pressure ahead of the bit in order to define a safe mud weight window for drilling and maintain wellbore stability. However, these rely on add-on instrumentation to the standards LWD/MWD configuration in order to work. Acoustic methods for gas detection leverage acoustic principles for kick detection. Pressure waves are generated in the mud and the travel time is monitored. Kicks can be detected by measuring the travel time. Gas will attenuate the mud velocity, increasing the travel time relative to pure mud alone. However, these methods also rely on the addition of instrumentation to the downhole assembly. There are other off-the-shelf, commercial kick detection technologies available at present. These includes systems such as the Landmark "Drillworks ConnectML", Weatherford's Early Kick/Loss Detection (EKLD) services, and tailor-made simulators which provide step-by-step guidance for well control in the event of a kick. However, each of these systems relies on additional downhole instrumentation or sensors.

1.4 NEED FOR A LOW-COST, EARLY DETECTION METHOD

Formation fluid influxes (i.e. kicks) pose persistent challenges and operational costs during drilling operations. Implications of kicks range in scale but cumulatively result in substantial costs that affect drilling safety, environment, schedule and infrastructure. To minimize these risks and impacts, it is critical that a kick is detected as early as possible. Early detection minimizes the kick influx volume received by the well, making the kick easier to suppress, reducing the stress on the well materials and machinery used to suppress the kick, and minimizing rig downtime. However, existing methods are either risk, e.g. mud logging, relying on physical circulation of mud returns to the rig floor and accompanying kick fluids/gases, or requires add-on software, tools, and instrumentation which add to operational costs.

2. EARLY KICK DETECTION USING GEOPHYSICAL MEASUREMENTS

2.1 RATIONALE

This method uses data from existing, downhole geophysical measurements to monitor the physical properties of fluid mixtures in the annulus. If the annulus has been invaded by formation fluids, the geophysical instrumentation will detect changes in the physical properties of the drilling fluid. Because this approach uses information on physical changes of drilling fluids to detect kicks, this approach requires using geophysical instrumentation that interacts with the fluids in the annulus. Drilling fluid and other materials (e.g. borehole cuttings, formation fluids) in the annulus interfere with geophysical instrumentation measurements. One method in which annular interference is reduced is by using instrument compensation. Compensation involves the use of multiple detectors at different spacings from the instrumentation measurement medium source. Compensation is achieved because the lateral depth-of-investigation by geophysical instrumentation into a geologic formation is primarily dependent on the source-receiver spacing. As the source-receiver spacing increases, the borehole radius, and therefore volume, which is measured by the geophysical instruments also increases. The increase in investigated volume means a greater lateral depth-of-investigation into the geologic formation. Once the investigated borehole volume extends beyond the annulus and into the geologic formation, it is then possible to subtract the annular effect from the total measurement, which assists in isolating the geologic formation measurements. However, it should be noted that greater borehole volume investigation also means a greater vertical investigation. The implication is that vertically-heterogeneous geologic features (e.g. thin beds, lenses, and formation boundaries) will be incorporated into measurements together. These mixed data will not accurately represent actual downhole conditions. It is therefore essential to consider complex lithological effects on the geophysical measurements in order to make an accurate assessment of both the annulus and the surrounding formation. Below the theory behind using commonly acquired LWD/MWD/SWD geophysical measurements, during modern drilling operations, is documented and their appropriateness for supporting early-kick detection near the bit is evaluated.

2.2 KICK DETECTION INSTRUMENTATION

Compensated geophysical instrumentation is used in virtually all LWD tool suites. Density, electrical resistivity, and acoustic velocity are among the compensated geophysical instrumentation that is typically used in LWD. Thus, geophysical data from compensated instrumentation should be readily available to provide kick detection. To determine if formation fluids have infiltrated the annulus (i.e. if a kick has occurred), this approach uses the physical property contrast that exists between unaltered drilling fluid and drilling fluid that has been mixed (or cut) with formation fluids. The contrast arises because the drilling fluid is typically quite different from the formation fluids, and therefore distinguishable using LWD technology. Drilling fluid compositions have formulated and well-constrained physical properties (e.g. resistivity, density, viscosity). The physical properties that offer the best versatility to account for any type of formation fluid influx (e.g. liquid petroleum, natural gas, brine) are density and electrical properties. These physical parameters are among the fundamental geophysical measurements made while drilling. The availability of such instrumentation allows for cost efficient and easy integration of this method into existing drilling rig ups.

The preferred instrumentation for use in this approach is:

- Bulk density
- Electrical resistivity
- Acoustic/sonic velocity

It should be noted that this approach is not limited to these tools. Other compensated geophysical instruments would also be satisfactory to employ this technique. However, the scope of the method described in this document will be limited to the preferred instrumentation listed above.

2.2.1 Density

Because a modest annular over-pressure is usually maintained during drilling, formation fluids are frequently less dense than drilling fluids. Liquid petroleum density is variable depending on its temperature, pressure, and composition. Liquid petroleum at sea level ranges from 0.6 to 0.9 g/cm^3 (Standing and Katz, 1942a; Ellis and Singer, 2007). Liquid petroleum density in the subsurface ranges from 0.4 to 0.7 g/cm^3 for pressures ranging from 70 to 20 MPa, respectively (England et al., 1987).

Petroleum density is characterized according to its composition in two primary ways. One is the specific gravity, G, which is the dimensionless ratio of the petroleum density relative to a reference density. For liquid petroleum, the reference is water at 15.6°C. For natural gas, the reference is air density at 15.6°C (Batzle and Wang, 1992). In addition to the specific gravity, the American Petroleum Institute (API) oil gravity number (°API) is used to classify crude oils according to their density (Batzle and Wang, 1992). The API oil gravity number for crude oil is given by the following equation:

Equation 1: API Oil Gravity Number Equation

$$°\text{API} = \frac{141.5}{G} - 131.5$$

Where G is the crude oil specific gravity (dimensionless). This relationship results in higher density crude oils having a lower °API number. Batzle and Wang (1992) reported densities for three different oil weights at three different formation pressures for a range of temperatures, (Table 1).

Table 1: Oil Densities (Batzle and Wang, 1992)

Oil Weight (°API)	Formation Pressure (MPa)	Temperature Range (°C)	Density Range (g/cm^3)
Light Oil (50°API)	0.1	20 to 100	0.7 to 0.85
	25	20 to 350	0.6 to 0.8
	50	20 to 350	0.6 to 0.85
Medium Oil (30°API)	0.1	20 to 100	0.85 to 0.9
	25	20 to 350	0.7 to 0.95
	50	20 to 350	0.7 to 0.95
Heavy Oil (10°API)	0.1	20 to 100	0.95 to 1.0
	25	20 to 350	0.75 to 1.05
	50	20 to 350	0.8 to 1.05

The lower oil densities reside at the higher range of the temperature scale. For formation temperatures and pressures that are observed in typical petroleum exploration wells, oil densities will be closer to the lower end of the range reported in Table 1.

Natural gas density also varies according to pressure, temperature, and composition. Below a critical depth, geologic pressure compresses natural gases into a liquid state, which significantly changes its density. Organic carbon natural gas density in gaseous state, composed of mostly methane at a wide range of temperatures and pressures, range from 0.01 to 0.7 g/cm^3 (Standing and Katz, 1942b; Lee et al., 1966, England et al., 1987; Batzle and Wang, 1992), while liquefied organic carbon natural gas density ranges from 0.4 to 0.7 g/cm^3 (Jensen and Kurata, 1969). Low-density gases have $G < 1.0$. For example, pure methane has a G of 0.56 (Batzle and Wang, 1992). In contrast, high-density gases have a G greater than 1.8 (Batzle and Wang, 1992).

Brine salinity also depends on local conditions. Fresh groundwater density will be ~1.0 g/cm^3, while 120,000 parts-per-million salt increases brine density to 1.1 g/cm^3 (Ellis and Singer, 2007). Similar to oil densities, the lower aqueous densities reside at the higher end of the temperature range. However, density stratification is expected to occur in brines in the subsurface, with brine density increasing with increasing depth. However, brines will be less dense than drilling fluids by necessity because drilling fluids have to hold back the formation pressure. A summary of groundwater densities as a function of salinity, pressure, and temperature is contained in Table 2.

Table 2: Aqueous Densities (Batzle and Wang, 1992)

Groundwater Salinity (ppm)	Formation Pressure (MPa)	Temperature Range (°C)	Density Range (g/cm^3)
0 (Fresh Groundwater)	9.81	20 to 250	0.85 to 1.0
	49	20 to 350	0.7 to 1.0
	98.1	20 to 350	0.8 to 1.1
20,000	9.81	20 to 250	0.9 to 1.1
	49	20 to 350	0.75 to 1.1
	98.1	20 to 350	0.85 to 1.1
150,000	9.81	20 to 250	0.95 to 1.1
	49	20 to 350	0.85 to 1.15
	98.1	20 to 350	0.9 to 1.15
240,000	9.81	20 to 250	1.05 to 1.2
	49	20 to 350	0.95 to 1.2
	98.1	20 to 350	1.0 to 1.2

Drilling fluid densities are prescribed based on need. As drilling depth increases, formation pressure also increases. In order to balance the pressure between the borehole and the formation, drilling mud density must also increase accordingly. Drilling mud densities are typically reported in terms of their specific weight (i.e. force per unit volume), with pounds-per-gallon (ppg) as the typical unit to describe for mud density. Water-based drilling fluid (i.e. water-based mud, WBM) densities are typically ≥ 1.0 g/cm^3 (Caenn et al., 2011), and range from approximately 1.1g/cm^3 (9.0 ppg) to 2.6 g/cm^3 (22.0 ppg). WBM densities are controlled by the concentration of inorganic metal salts (e.g. potassium chloride, calcium chloride, calcium bromide, barium sulfate) dissolved in solution. Oil-based drilling fluids (i.e. oil-based muds, OBMs) are an emulsion of water and an organic solvent (Bourgoyne et al., 1986), usually #2 diesel fuel or mineral oil. Because the organic solvent phase of an OBM is less dense than water, OBMs can reach a lower density than WBMs. OBM densities are typically ≥ 0.8 g/cm^3 (Caenn et al., 2011), and range from approximately 0.8 g/cm^3 (7.0 ppg) to 2.6 g/cm^3 (22.0 ppg). OBM densities can be controlled by the oil:water ratio, as well as the weighting salt concentration. Gases, mists, and foams are also used as drilling fluids. However, virtually all oil and gas drilling will encounter significant formation pressures that will require the use of either WBMs or OBMs.

Effects of Formation Fluid Influx on Drilling Fluid Density

Formation fluid mixing with drilling fluid will generate a clear density contrast when compared to unaltered drilling fluid, enabling kick detection by the density tool. Gamma density instruments similar to those that are deployed in the borehole as part of the while-drilling tool suites have been used to detect multiphase flow in pipes (Hewitt, 1978). The magnitude of the density contrast will depend on the intrinsic formation fluid properties (e.g. composition, density), the volume of formation fluid entering the borehole, as well as the intrinsic drilling fluid properties (e.g. composition and density). The density contrast will be drilling fluid dilution

because of formation fluid mixing, which will alter the drilling fluid density. The bulk density of a mixture is given by Equation 2, which will be used to model the bulk density of a mixture of drilling fluid and kick fluid as a function of volume fraction.

Equation 2: Kick Fluid:Drilling Fluid Mixture Density Modeling

$$\rho = \varphi_A\rho_A + \varphi_B\rho_B + .. + \varphi_n\rho_n$$

Where φ_n is the volume fraction (dimensionless) of the nth mixture component, and ρ_n is the bulk density (g/cm^3) of the nth mixture component.

A graphical representation of the predicted effects on mixture density because of formation fluids mixing with water-based and oil-based drilling fluids is presented in Figure 1. The upper plot shows the relationship between bulk density and volume fraction of three different kick fluids for a borehole drilled with a water-based mud. The lower plot shows the relationship between bulk density and volume fraction of three different kick fluids for a borehole drilled with an oil-based mud. The three kick fluids for both scenarios are brine (blue plot), natural gas (red plot), and oil (green plot). Presuming drilling with an overpressure in the borehole to prevent a kick from occurring, the drilling mud density for all instances will be greater than the kick fluid density. This is exhibited in the plot trends. As the volume fraction of kick fluid increases, the density of the drilling fluid:kick fluid mixture decreases, approaching the density of the pure kick fluid. These results imply that, provided that overpressure drilling is conducted, infiltration of a kick will decrease the density of the drilling fluid in virtually all instances. A summary of the predicted effects on mixture density because of formation fluid mixing with drilling fluid is provided in Table 3.

Key Points

- When conducting overbalanced drilling, drilling fluid density will be greater than formation fluid density. Thus, formation fluid mixing with drilling fluid will result in a mixture whose density is lower than the pure drilling fluid and greater than the pure formation fluid
- Drilling fluid density will be affected by a formation fluid influx to the extent that it will be measureable using LWD/MWD density instrumentation

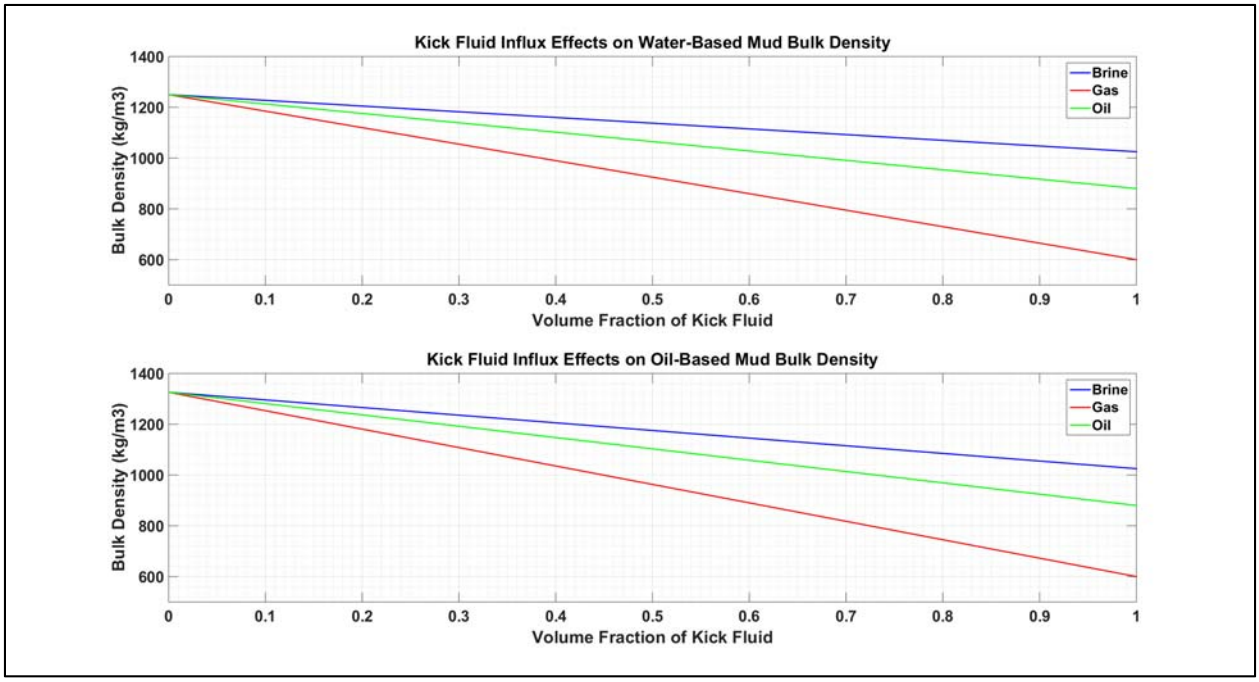

Figure 1: Effects of kick fluid mixing on drilling fluid bulk density.

Table 3: Predicted Kick Fluid Effects on Drilling Fluid Density

Drilling Fluid Base	Typical Drilling Fluid Density Range (g/cm^3)[ppg]	Formation Fluid (Kick)		
		Water (1.0 to 1.1 g/cm^3)	Liquid Petroleum (0.6 to 0.85 g/cm^3)	Natural Gas (0.01 to 0.7 g/cm^3)
Water	1.0 to 2.6 [8 to 22]	Variable, depending on drilling fluid weight. Typically should be a density decrease because the drilling mud density should be higher than the formation fluid	Density Decrease	Density Decrease
Oil	0.8 to 1.8 [7 to 22]	Variable, depending on drilling fluid weight. Typically should be a density decrease because the drilling mud density should be higher than the formation fluid	Variable, depending on drilling fluid weight. Typically should be a density decrease because the drilling mud density should be higher than the formation fluid	Density Decrease

2.2.2 Electrical Resistivity

Formation fluid electrical properties vary widely and reside at the extrema of the material electrical property continuum. Liquid petroleum and natural gases are mixtures of hydrocarbons, which are intrinsic electrical insulators, and have electrical resistivity values of approximately 2 x 10^{14} ohm-meters (Ω-m) (Ellis and Singer, 2007). In contrast, brine is an electrical conductor, whose electrical resistivity depends on the electrolyte content of the solution, with values ranging from 0.06 Ω-m for high-salt content brines (200,000 ppm salt) to 3.4 Ω-m for low-salt content brines (2,000 ppm) (Ellis and Singer, 2007). Freshwater electrical resistivity spans a wide range. Pure water is an electrical insulator, with a resistivity of approximately 2 x 10^{14} ohm-meters (Ellis and Singer, 2007). However, groundwater will contain dissolved or suspended electrolytes, which lower the electrical resistivity significantly to values in the range of several to 100 Ω-m (Urish, 1983; Samouëlian et al., 2005).

Drilling fluids are a mixture of a base fluid and additives with widely varying electrical properties. Oil-based drilling fluids are composed of an electrically-insulating base fluid (e.g. #2 diesel fuel or mineral oil), but are weighted with electrically-conducting salts, such as calcium chloride and sodium chloride. A minority fraction of oil-based drilling fluid is water so that the weighting salts can dissolve. The immiscible oil and aqueous phases are emulsified using surfactants, which disperses the electrolytic aqueous phase throughout the mixture, moderating its electrical properties. Electrical resistivity as a measurement depends on physical parameters, such as pressure, temperature, and measurement frequency. The electrical resistivity of oil-based drilling muds additionally depends on mixture composition, such as desired fluid weight and oil-water ratio. Because factors such as fluid density and oil:water ratio vary according to the needs of the particular well being drilled, a wide range of electrical resistivities exist for oil-based drilling fluids, ranging from as low as 500 Ω-m up to 30,000 Ω-m (Patil et al., 2010; Wang et al., 2003).

Similar to oil-based drilling fluids, the desired water-based drilling fluid density is achieved by adding salts, clays, and other high-density minerals (e.g. bromide and chloride salts). These salts dissolve in the aqueous base fluid and form an electrolytic solution that is an electrical conductor. The result is a mixture whose electrical resistivity ranges from less than 1.0 Ω-m to approximately 15 Ω-m (Overton and Lipson, 1958; Schnoebelen et al., 1995; Wang et al., 2003; Patnode, 1949; Lamont, 1957).

Effect of Formation Fluid Influx on Drilling Fluid Resistivity

Petroleum-based formation fluid influx effects are easier to predict when compared to the effects of an aqueous-based formation fluid influx. Because of the strong electrical insulation by petroleum-based formation fluids, a petroleum influx will result in a clear electrical resistivity increase for both OBM and WBM. Although, based on the relatively low electrical resistivity exhibited by WBM, electrical insulation effects from petroleum-based formation fluids are expected to be more apparent in a WBM than an OBM.

Aqueous formation fluid influx effects are not as easily predicted, as they depend on the electrolyte concentrations of both the formation fluid and the drilling fluid. Because formation brines are relatively strong electrical conductors, with resistivity values ranging from 0.01 to 1.0 Ω-m depending on temperature and composition (Archie, 1942; Ucok et al., 1980; Nesbitt, 1993), they are expected to lower OBM resistivity when they influx. However, WBMs are already strong electrical conductors, thus the mixing of a conductive formation fluid with a

conductive drilling fluid will present a nuanced effect. A summary of the predicted effects on mixture electrical resistivity because of formation fluid mixing with drilling fluid is presented in Table 4.

Table 4: Predicted Kick Fluid Effects on Drilling Fluid Electrical Resistivity (Overton and Lipson, 1958; Schnoebelen et al., 1995; Patil et al., 2010; Wang et al., 2003; Urish, 1983; Samouëlian et al., 2005; Ellis and Singer, 2007; Patnode, 1949; Lamont, 1957)

Drilling Fluid Base	Typical Drilling Fluid Electrical Resistivity Range (Ω-m)	Formation Fluid (Kick)			
		Freshwater (Electrical Resistivity ≈ 1 to 10 Ω-m)	Brine (Electrical Resistivity ≈ 0.06 to 3.4 Ω-m)	Liquid Petroleum (Electrical Resistivity ≈ 2.0 x 10^{14} Ω-m)	Natural Gas (Electrical Resistivity ≈ 2.0 x 10^{14} Ω-m)
Water	0.1 to 15	Varies depending on drilling fluid and freshwater compositions	Varies depending on drilling fluid and brine compositions	Resistivity increase	Resistivity increase
Oil	1,000 (no frequency) 2,000 to 30,000 (at low frequencies) 500 to 10,000 (at high frequencies)	Resistivity decrease	Resistivity decrease	Resistivity increase	Resistivity increase

Previous Research on Electrical Resistivity and Drilling Fluid

Patil et al. (2010) studied the resistivity of OBMs for frequencies between 1–100 MHz at temperature ranging from 20–60°C (below the flashpoint of the oil in the OBMs) for different oil-wt% content, water-wt% content, and $CaCl_2$-wt% content. They found the following on resistivity of OBMs:

1. Resistivity decreases with increasing frequency and increasing temperature
2. Resistivity increases with increase in oil/water ratio
3. Resistivity increases as salt content decreases
4. No specific relation could be found on how water content of the mud affects resistivity. A decreasing trend in resistivity could be seen with increasing water vol% though in a scattered manner.

Sample parameters from Patil et al. (2010) are presented in Table 5. Results from Patil et al. (2010) are presented in Table 6.

Table 5: OBM Samples (Patil et al., 2010)

Sample	Oil-Base Mud	Oil Wt%	$CaCl_2$ Wt%	OWR	Sample Type
1	Sample 1	40	3.3	71/29	Prepared
2	Sample 2	60	6.6	79/21	Prepared
3	Sample 3	25	5.0	59/41	Prepared
4	Sample 4	45	5.0	60/30	Prepared
5	Sample 5	45	15.0	71/29	Prepared
6	Sample 6	40	6.3	72/28	Prepared
7	Sample 7	55	3.7	86/14	Prepared
8	Sample 8	70	4.7	86/14	Prepared
9	Sample 9	-	-	-	Field Sample
10	Sample 10	-	-	-	Field Sample
11	Sample 11	-	-	-	Field Sample
12	Sample 12	-	-	-	Field Sample
13	Sample 13	-	-	-	Field Sample
14	Sample 14	42	2.9	66/34	Field Sample
15	Sample 15	-	-	-	Field Sample
16	Sample 16	68	19.0	78/22	Field Sample
17	Sample 17	-	-	-	Field Sample
18	Sample 18	-	-	-	Field Sample
19	Sample 19	66	24.67	80/20	Field Sample

Table 6: Measured Resistivity Data of Different Samples at Various Temperatures and 10 MHz (Patil et al., 2010)

Sample	Oil Wt%	$CaCl_2$ Wt%	OWR	ρ at 20°C*	ρ at 30°C*	ρ at 40°C*	ρ at 50°C*	ρ at 60°C*
1	40	3.3	71/29	2.69	2.37	1.79	1.27	0.937
2	60	6.6	79/21	8.36	5.82	3.47	2.41	1.62
3	25	5.0	59/41	0.92	0.92	0.871	0.76	0.653
4	45	5.0	60/30	2.95	2.75	2.53	2.01	1.59
5	45	15.0	71/29	5.44	4.25	3.99	3.53	3.06
6	40	6.3	72/28	2.57	2.49	2.04	1.86	1.53
7	55	3.7	86/14	4.00	2.93	2.04	1.41	0.894
8	70	4.7	86/14	4.26	3.19	2.22	1.48	1.07
9	-	-	-	2.46	2.07	1.49	1.10	0.749
10	-	-	-	0.926	0.926	0.926	0.892	0.81
11	-	-	-	0.696	0.631	0.56	0.512	0.455
12	-	-	-	0.943	0.853	0.733	0.732	0.659
13	-	-	-	0.926	0.779	0.741	0.671	0.603
14	42	2.9	66/34	0.856	0.856	0.856	0.853	0.853
15	-	-	-	0.609	0.598	0.574	0.574	0.574
16	68	19.0	78/22	2.30	1.90	1.67	1.67	1.45
17	-	-	-	0.594	0.571	0.541	0.522	0.522
18	-	-	-	0.305	0.305	0.273	0.254	0.222
19	66	24.67	80/20	0.603	0.566	0.545	0.527	0.527

* x 10,000 Ω-m

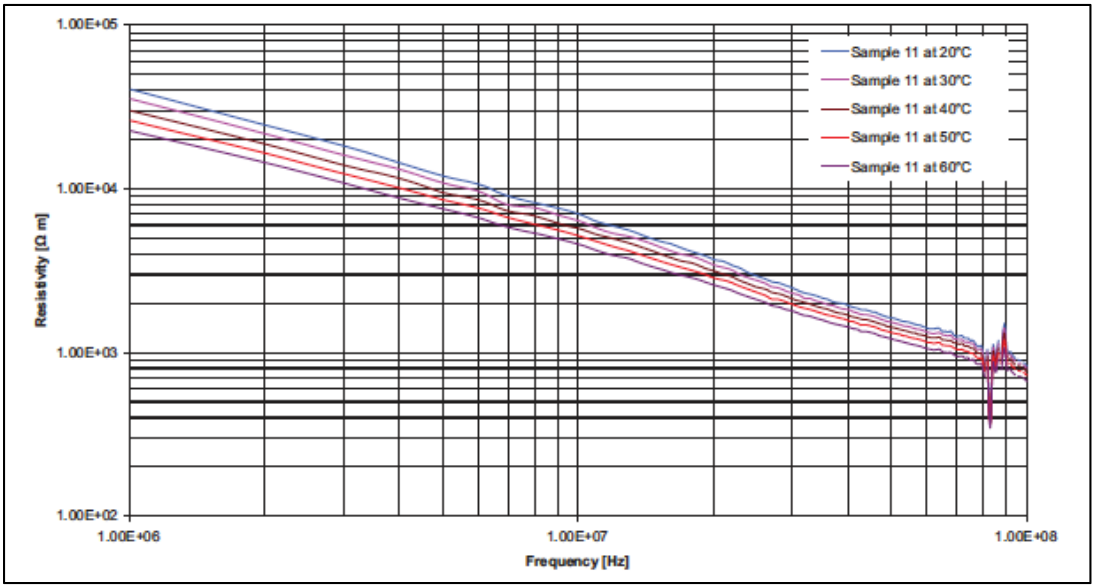

Figure 2: Temperature effect on resistivity – Sample 11 (Patil et al., 2010).

Electrical resistivity of a single sample (Sample 11) is plotted as a function of the measurement frequency for five different temperatures in Figure 2. The units for resistivity are ohm-meters and the units for frequency are Hertz. As measurement frequency increases, the resistivity measurement decreases. For the same measurement frequency, the resistivity measurement decreases with increasing temperature. As measurement frequency increases, the differences between the individual resistivity measurements decrease, suggesting that temperature effects on the resistivity measurement diminish as sampling frequency increases.

The shallow resistivity measurement (i.e. a short source:receiver spacing) is the preferred electrical resistivity measurement for detecting kicks.

To detect an influx using electrical resistivity, it is necessary to establish rules based on known values for drilling fluid resistivity and kick fluid resistivity. Based on those rules, a model of the expected signal response was built with respect to depth, for influx and non-influx conditions, taking into consideration the various physical parameters that affect the resistivity log so that a difference in response would indicate influx.

Bryant et al. (1991) tested a formation fluid influx detection technique which monitors electrical resistivity and acoustic responses of annular MWD measurements. Gas was the primary formation fluid tested in the experiments, but both freshwater and salt water were also tested. Both OBM and WBM were used in the experiment. Table 7 contains data related to the electrical resistivity portion of their experiments. For the 14 gas kicks contained in Table 7, the kicking fluid was nitrogen gas. “Baseline resistivity” represents the gas-free drilling mud resistivity and “influx resistivity measurements” represents resistivity values after gas injection. For kick detection, a sustained change greater than one standard deviation from mean of drilling mud was indicative of influx. Gas influx could not be detected for gas concentrations below 8.5 scf/bbl. Above that concentration, influx resistivity values increased slightly for gas-cut mud, increased very significantly for freshwater influx, and significantly reduced for salt water influx. The resistivity of gas-cut mud is proportional to gas volume.

Table 7: Gas Influx Test (Bryant et al., 1991)

Kick	Surface Injection Volume (scf)	Injection Time (minutes)	Injection Rate (scf/min)	Pump Rate (bbl/min)	Gas Concentration (scf/bbl)	Surface Gas/Mud Ratio	Downhole Gas Concentration (vol%)	Baseline Resistivity Measurements (Ω)	Influx Resistivity Measurements (Ω)	Resistivity Measurement-Derived Gas Concentration (vol%)
28	186	3.17	59	7.78	7.5	1.3	1.9	0.65	0.66	1.5
29	776	12.00	65	7.78	8.3	1.5	2.1	0.66	0.67	1.5
25	1060	12.60	84	6.21	13.5	2.4	3.5	0.60	0.62	3.3
27	397	3.10	128	7.78	16.5	2.9	4.2	0.67	0.70	4.5
24	1060	6.27	169	6.21	27.2	4.8	6.9	0.60	0.65	8.3
26	780	3.17	246	7.78	31.6	5.6	8.1	0.67	0.72	7.5
19	789	3.17	249	7.78	32.0	5.7	8.2	0.66	0.72	9.1
23	1314	6.27	210	6.21	33.7	6.0	8.6	0.65	0.72	10.8
22	809	3.10	261	6.21	42.0	7.5	10.7	0.62	0.73	17.7
21	1017	3.08	330	6.21	53.2	9.5	13.6	0.65	0.74	13.8
20	1155	3.17	364	5.98	60.9	10.9	15.6	0.66	0.76	15.2
30-1	428	0.95	451	5.98	75.4	13.4	19.2	0.65	0.79	21.5
30-2	451	0.95	475	5.98	79.4	14.1	22.0	0.65	0.80	23.1
30-2	428	0.83	516	5.98	86.3	15.4	20.3	0.65	0.80	23.1
31	15 bbl	2.00	Injection of Salt Water				N/A	0.65	0.14	N/A
32	19 bbl	3.22	Injection of Fresh Water				N/A	0.52	8.31	N/A

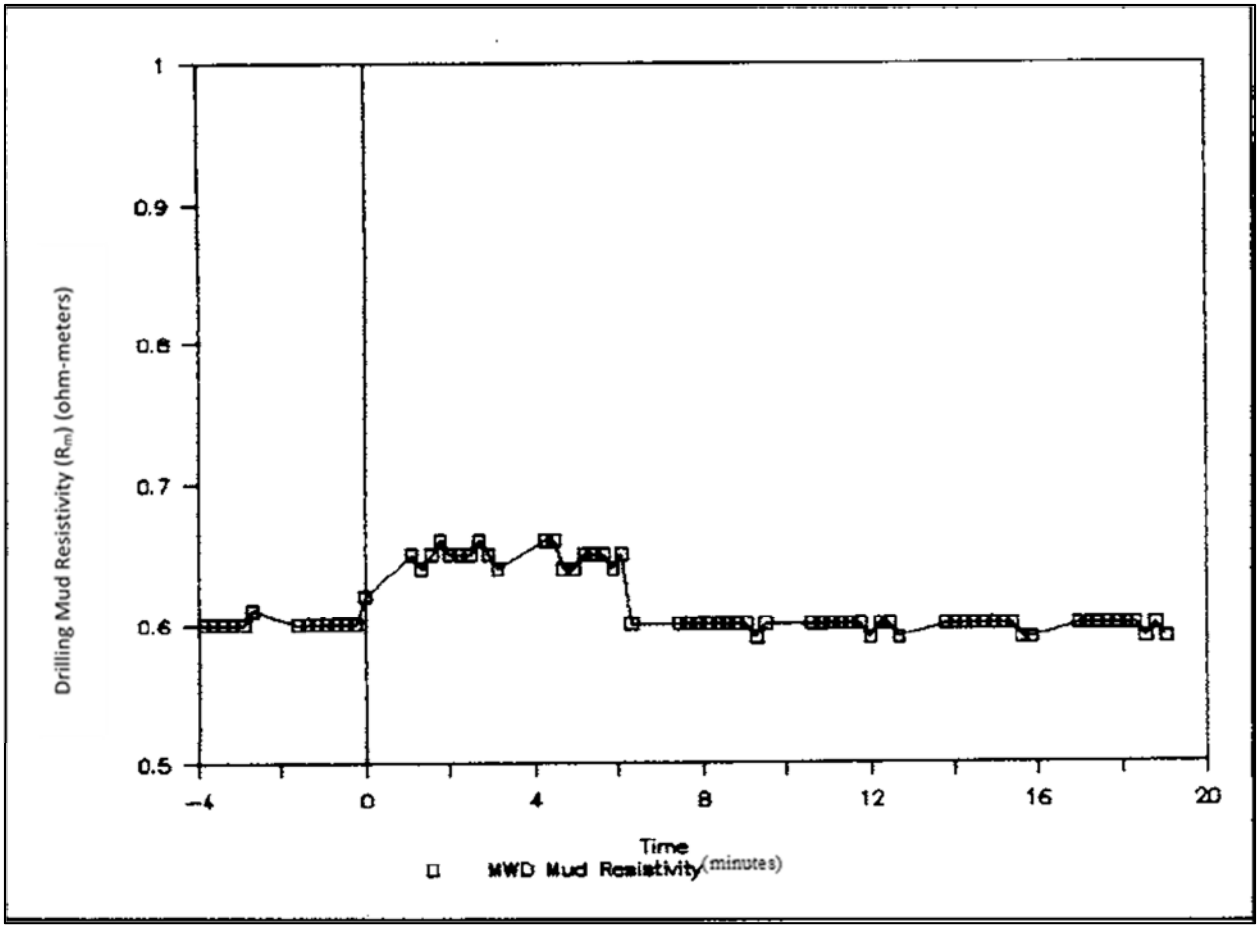

Figure 3: Gas influx detection using a downhole MWD mud resistivity sensor (Bryant et al., 1991).

Figure 3 shows drilling mud electrical resistivity (R_m) affected by a gas influx plotted as a function of time. The units for electrical resistivity are ohm-meters, the units for time are minutes. At time = 0, a gas volume of 1,060 scf at a concentration of 27.2 scf/bbl was injected into the mud. The mud resistivity increases as gas moves past the downhole sensor. The rate of detection using resistivity measurements is also shown in Table 8. For different gas concentration values, influx was detected within 0.5 to 3 min of kick initiation. Hewitt (1978) describes a method to detect two-phase flow (e.g. gas in liquid) in pipes as a function of gas void fraction using electrical impedance methods.

Table 8: Detection Times for Downhole Mud Resistivity (Bryant et al., 1991)

Kick	Gas Concentration (scf/bbl)	Detection Time (minutes)			
		0.20 Hz	0.40 Hz	0.60 Hz	Resistivity Measurements
28	7.5	-	-	3 +	-
29	8.3	8	4.5	2.0	-
25	13.5	5.5	6.5	1.5	1.5
27	16.5	4	5	1.5	3
24	27.2	5.5	4	1.5	1.5
26	31.6	4.5	2	1.5	1.5
19	32.0	8	8	1	1
23	33.7	1+	3.5	1.5	1.5
22	42.0	2+	2	1.5	1
21	53.2	2	4+	1+	0.5
20	60.9	2+	4	1.5	0.5
30-1	75.4	2	2	1.5	0.5

Key Points

- Because of the distinctive electrical properties for the various kick fluids, electrical resistivity measurements show great promise for both detecting and differentiating kick fluids
- Previous work on the use of annular resistivity measurements for kick fluid detection shows that MWD instrumentation is sufficiently sensitive to detect both gaseous and aqueous kick fluids in a timely manner
- Based on the results from the previously published work, and the evidence that electrical methods are used to detect two-phase flow in pipes, changes in drilling fluid electrical properties because of mixing with formation fluid are sensible by the LWD/MWD instrumentation in the annulus

2.2.3 Acoustic Velocity

Acoustic logging is the recording of acoustic velocities or the time required for a sound wave to traverse a definite length of formation (Tixier et al., 1958). For a given geologic formation, the travel time is inversely proportional to the speed-of-sound. Acoustic logging provides a rock's acoustic properties such as the velocity and rate of attenuation for different modes of sound waves. The acoustic velocity through a material is a function of a material's intrinsic elastic properties. Elastic properties describe a material's resistance to deformation. Examples of these material properties include the bulk modulus, which describes a material's resistance to uniform compression, and the shear modulus, which describes a material's rigidity. Regarding all states of matter, incompressible and/or rigid materials have higher elastic moduli than softer materials.

For illustration, the compressional wave, or *p*-wave, velocity for a given material is given by Equation 3:

Equation 3: Compressional Velocity Equation

$$V_p = \sqrt{\frac{K + \frac{4}{3}\mu}{\rho}}$$

Where V_p is the compressional velocity (meters per second), K is the bulk modulus (newtons per square meter (pascals)), μ is the shear modulus (pascals), and ρ is the bulk density (grams per cubic centimeter). Because fluids (e.g. gases and liquids) cannot propagate shear waves, their shear moduli are zero. This causes the compressional wave velocity in fluids to be a function solely of the bulk modulus and density.

Similar to electrical resistivity, formation fluid elastic properties, and hence acoustic properties, vary according to temperature, pressure, and material composition (Thomas et al., 1970). Natural gas bulk moduli decrease with increasing temperature, and increase with increasing pressure (Batzle and Wang, 1992). At the same low temperatures and pressures, natural gas bulk moduli significantly differ with respect to molecular weight; with high specific gravity gases (G = 1.2) possessing a much higher bulk modulus than lower specific gravity gases (G = 0.6)(Batzle and Wang, 1992). As temperature increases, the bulk modulus converges to a common value, regardless of gas specific gravity (Batzle and Wang, 1992).

Crude oil acoustic velocity increases with increasing fluid density (lower °API or higher G), increases with increasing pressure, and increases with decreasing temperature (Wang et al., 1990). Because of the high pressures present in geologic formations, natural gases can dissolve into crude oils. Crude oil with a dissolved gas phase is referred to as “live” oil, whereas crude oil without a dissolved gas phase is referred to as “dead” oil. Crude oil containing dissolved gas has a lower acoustic velocity when compared to crude oil containing no gas (Batzle and Wang, 1992).

Aqueous formation fluid (e.g. brine and fresh groundwater) elastic properties are influenced by the same physical variables as crude oil and natural gas. Aqueous fluid acoustic velocity increases with increasing salt concentration or decreasing temperature. Aqueous fluid velocity increases isothermally with increasing pressure (Batzle and Wang, 1992).

Aqueous formation fluids can also dissolve a gas phase. The amount of gas dissolved is dependent on the pressure and the brine’s salt content. A small amount of dissolved gas significantly decreases the mixture’s acoustic velocity. The observed velocity decrease from gas dissolution is less pronounced at higher pressures for the same gas concentrations. Greater gas concentrations are required to elicit the same velocity reduction at higher pressures (Batzle and Wang, 1992).

Effect of Formation Fluid Influx on Acoustic Velocity

An influxing formation fluid’s bulk modulus is critical for predicting how a drilling fluid’s acoustic properties change during a kick. Changes to the mixture’s bulk modulus will be the most direct way to alter the acoustic properties of a fluid. This phenomenon is demonstrated by Wood’s equation (1941) (used in Batzle and Wang, 1992; Carcione and Poletto, 2000):

Equation 4: Wood's Equation

$$\frac{1}{K_m} = \frac{\varphi_A}{K_A} + \frac{\varphi_B}{K_B} + \cdots \frac{\varphi_n}{K_n}$$

Where K_m is the mixture's bulk modulus, φ_n is the individual mixture component's nth term volume fraction, and K_n is the individual mixture component's nth term bulk modulus.

Knowledge of the kicking fluid's elastic properties and volume fraction will permit a velocity change prediction. The bulk moduli of the most basic formation fluids are summarized in Table 9.

Table 9: Formation Fluid Bulk Moduli (Batzle and Wang, 1992)

Formation Fluid	Bulk Modulus (MPa)
Fresh Groundwater	500 to 3,000
Light Brine Groundwater (150,000 ppm)	1,000 to 3,500
Heavy Brine Groundwater (300,000 ppm)	2,000 to 5,000
Light Liquid Petroleum (50° API)	100 to 2,000
Medium Liquid Petroleum (30° API)	200 to 2,500
Heavy Liquid Petroleum (10° API)	300 to 3,500
Light Hydrocarbon Natural Gases (G = 0.6)	10 to 200
Heavy Hydrocarbon Natural Gases (G = 1.2)	25 to 600

Note: Pressure range is 0.1 MPa, 25 MPa, and 50 MPa. Temperature range is 0°C to 350°C.

Each kick fluid's bulk moduli spans a relatively wide range. A kick fluid's bulk modulus decreases as temperature increases. Thus, temperature becomes the commanding variable in predicting a kick fluid's effects on a drilling fluid's elastic properties, especially regarding liquid petroleum. With the knowledge that temperature will ultimately control a kick fluid's bulk modulus, the local geothermal gradient becomes the critical factor in predicting a kick fluid's effect on drilling fluid's elastic properties. Geothermal gradients typically range from 20°C/km to 100°C/km. Using a subsurface temperature of 100°C as a benchmark, the only formation fluid whose bulk modulus is near to a drilling fluid's bulk modulus is a concentrated brine (e.g. 300,000 ppm brine). It is uncommon for naturally-occurring brines to reach such a concentration. Batzle and Wang (1992) reported salinities for deep formation brines near the Gulf of Mexico whose salinities approached, and at times exceeded, 300,000 ppm. However, concentrations reaching this level were achieved because of interbedded salt layers. Groundwater salinity is expected to be much less in basins composed of clastic sediments (Batzle and Wang, 1992). With high salinity being a rare occurrence in on-shore wells, the implication is that for on-shore wells drilled below a critical depth, a depth which is dependent on the geothermal gradient, any formation fluid influxing into the annulus will have a lower bulk modulus than the drilling fluid, and hence, will decrease the drilling fluid's acoustic velocity. For a typical geothermal gradient, the 100°C benchmark subsurface temperature corresponds to a well depth of approximately 1 to 5 km (~3,300 to 16,000 ft), a range which is well-within the nominal depth range of a petroleum

exploration well. For basins where bedded salts are known, or presumed, to occur, (e.g. offshore Gulf of Mexico) the effects of formation brine salinity must be considered in the prediction of formation fluid effects on drilling fluid elastic properties.

Table 10: Drilling Fluid:Kick Fluid Mixture Modeling Parameters (Carcione and Poletto, 2000)

Drilling Fluid Constituent	Bulk Modulus (GPa)	Density (g/cm^3)	Volume Fraction
Clay (viscosifier)	36	2.5*	0.03
Barite (weighting material for water-based mud)	55	4.2	0 to 0.064 (depending on depth)
Itabarite (weighting material for oil-based mud)	80	5.1	0.056 to 0.104 (depending on depth)
Water	3	1.0	Remainder of total volume
#2 Diesel Fuel	1.5	0.832	Remainder of total volume

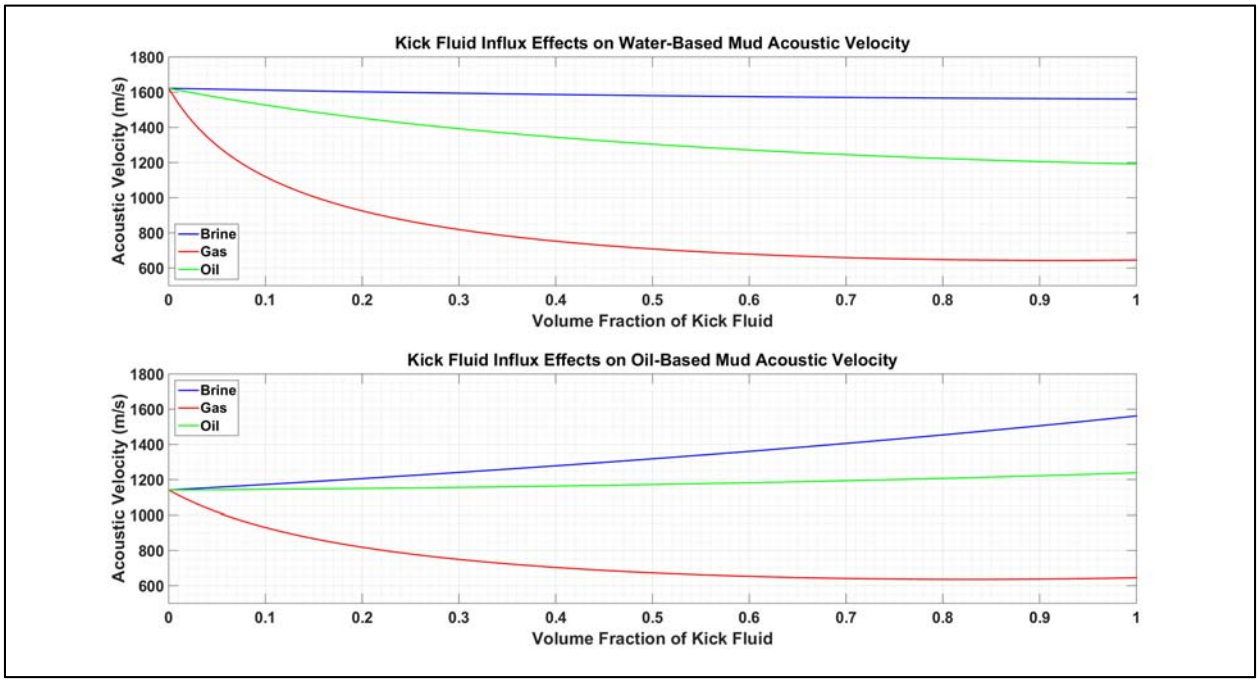

Figure 4: Effects of kick fluid mixing on drilling fluid acoustic/sonic velocity.

A graphical representation of the predicted effects on mixture acoustic velocity because of formation fluids mixing with water-based and oil-based drilling fluids is presented in Figure 4. In Figure 4, the upper plot shows the relation between acoustic velocity and volume fraction of three separate kick fluids for boreholes drilled with a water-based drilling fluid. The bottom plot shows the relation between the acoustic velocity and the volume fraction of three separate kick fluids for boreholes drilled with an oil-based drilling fluid. For both plots, the three separate kick fluids are: 8.6 ppg (1.025 g/cm^3) brine (blue plot), 0.6 G natural gas (red plot), and 0.88 G (30° API) oil (green plot). Although a borehole overpressure while drilling is presumed, the controlling variable in the velocity contrast between kick fluid and drilling fluid is each fluid's bulk modulus. Water-based and oil-based drilling fluid recipes from Carcione and Poletto, (2000) were used with Wood's equation (Equation 4) to model the acoustic velocity for each drilling fluid:kick fluid mixture. Table 10 presents these recipes. The results show good agreement with other published drilling fluid acoustic velocities (Crowo, 1990). For water-based drilling fluid, pure kick fluids display a lower acoustic velocity than pure drilling fluid, which results in drilling fluid:kick fluid mixture acoustic velocities being lower than pure water-based drilling fluid velocity. For oil-based fluids, oil and brine acoustic velocities are both greater than oil-based drilling fluid acoustic velocity, resulting in drilling fluid:kick fluid mixture velocities to be greater than pure oil-based drilling fluid velocity. Because of the exceedingly low bulk modulus for natural gas, drilling fluid:natural gas mixtures show a sharp velocity decrease even when natural gas volume fraction is low. A summary of the predicted effects on mixture acoustic velocity because of formation fluid mixing with drilling fluid is presented in Table 11.

Table 11: Predicted Kick Fluid Effects on Drilling Fluid Acoustic Velocity (Carcione and Poletto, 2000; Batzle and Wang, 1992)

Drilling Fluid Base	Typical Drilling Fluid Acoustic Velocity Range, m/s	Formation Fluid (Kick)		
		Aqueous Formation Fluid (Acoustic Velocity ≈ 600 to 1,900 m/s)	Liquid Petroleum (Acoustic Velocity ≈ 900 to 2,300 m/s)	Natural Gas (Acoustic Velocity ≈ 200 to 750 m/s)
Water	1,300 to 1,600	Variable depending on salinity, decrease occurs beyond a critical depth	Variable, decrease occurs beyond a critical depth	Velocity decrease
Oil	1,000 to 1,300	Variable depending on salinity, decrease occurs beyond a critical depth	Variable, decrease occurs beyond a critical depth	Variable depending on gas saturation, critical saturations depend on pressure, likely decrease due to bulk modulus reduction

Key Points

- Acoustic/sonic velocity measurements for kick detection will be drilling-fluid-dependent and should be interpreted on a case-by-case basis
- A significant decrease in drilling fluid velocity signifies a gas kick fluid

- Based on the findings presented here, drilling fluid mixing with formation fluid produces a composite fluid whose acoustic properties are significantly different from either pure fluid. This property contrast will be sensible by LWD/MWD acoustic velocity instrumentation

2.3 SIGNAL PROCESSING

2.3.1 Data Compression

LWD instrumentation generates a significant amount of data, some of which are needed in real-time for monitoring, decision-making, and safer drilling activity. Available data transmission methods with limited transmission rates, such as mud pulse telemetry, would benefit from data compression in order to ensure delivery of all essential data in real-time.

In data compression, measurements, signals and/or images generated are represented with less bits than the original in order to improve transmission time and save storage space and its associated costs. After transmission the data are recovered through decompression.

The indices for measuring compression algorithm performance are the compression ratio, the amount of data distortion, and the time cost, which is a factor of the computational complexity. For LWD data, the lossy form of compression based on discrete wavelet transforms (DWT) is commonly used. It has been found to be reliable and to perform at high compression ratio with low error in LWD data (Li, 1996).

Lossless Compression Algorithms

In lossless compression just as the name implies, the original signal is reduced into a smaller size and data are recovered with no information loss. Compression is achieved by the identification and elimination of statistical redundancy.

Lossy Compression Algorithms

Lossy compression provides an effective means of data compression whereby instead of an exact replication, the original signal is approximated within acceptable degree of accuracy. The degree of data compression is proportional to the approximation, and since these algorithms have higher compression. Therefore, higher compressions result in higher approximation (e.g. more “lossy-ness”). The main points for lossy compression are:

- Data recovery with some information loss
- Higher compression ratio
- Lower computational complexity
- Useful where real-time delivery is more important than accuracy (data distortion does not adversely affect data analysis)

2.3.2 Data Transmission

Transmission methods for while-drilling data vary widely in their techniques and complexity. More modern techniques, such as wired drillstring or electromagnetic telemetry, permit a relatively high data through-put rate, and present a significant advantage over mud-pulse telemetry. However, modern techniques suffer from implementation difficulties which present

the risk of stopping drilling or losing the ability to transmit data, which limit their use in the field.

Mud pulse telemetry, while not as efficient at data transmission as more modern methods, is the most reliable technique currently available and, hence, is more widely used when real-time data are demanded while-drilling. Because the probability is high that exploration wells will be using mud pulse telemetry exclusively, the scope of this project will be limited to focusing on mud pulse telemetry for data transmission. If a specific drilling project uses a data transmission method that permits a greater data transmission rate, then the kick detection technique described here will perform better than what is described in this document, as the data transmission rate is the most inefficient portion of the kick detection process.

Mud Pulse Telemetry

This is the most common method of data transmission. The basic principle used is to create pressure pulses by restricting the flow of mud in the drillpipe. The pulse is attenuated as it is transmitted through the drilling mud and partially reflected to the surface where they are received by pressure sensors. As a result of attenuation, the energy of the pressure wave received at the surface is a fraction of the energy emitted by the pulser downhole. The signals are then processed at the surface to decode useful information.

Currently, the tools can generate three types of pulses:

1. Positive Pulse - a valve is used to restrict mud flow in the drillpipe resulting in an increase in pressure that propagates to the surface
2. Negative Pulse - valve releases mud from the drillpipe into the annulus casing using an annular venting system. This causes a decrease in pressure that can be detected at the surface.
3. Continuous Wave - the valve is gradually closed and opened to generate sinusoidal pressure fluctuations in the mud

The MWD tool consists of a pulsing assembly or modulator that generates the pressure pulse through the mud. The most advanced means of pulse creation is by a mud siren. The mud siren includes a rotator that spins and alternately releases or blocks mud flow over a stator. A continuous mud-wave is transmitted within the drilling fluid and as the rotator spin rate changes, there is a phase shift in the sinusoidal wave. This shift is measured and decoded into bits. The phase of the signal is changed through frequency modulation to convert bit words that represent information from various sensors.

Data Rate: Data rates through mud pulse telemetry are typically 6 to 10 bps and the rate decreases to between 1.5 to 3 bps as borehole depth increases (about 35,000 to 40,000 ft)

Limitations

1. Surface-to-downhole communication through mud pulse telemetry is performed by changing drilling parameters such as speed of drillstring rotation or mud flowrate. These changes interrupt the drilling process and result in rig downtime.
2. Data transmission rate reduces with increased depth, making it likely unsuitable for ultra-deep wells

3. Signal is easily affected by interfering noise signals (from drilling, mud pumps etc.)
4. For highly compressible drilling fluids such as OBM, the signal is more attenuated for higher frequency data transmission

2.3.3 Data Filtering

Once the geophysical measurement is received at the surface, the data undergo a series of filter processes. The first process is the separation of the annular data from the total measurement signal. This process extracts the portion of the total signal that represents the state of the annulus. Once the annular portion of the total measurement signal has been isolated, the annular data are continuously concatenated into a data string.

The annular data are then processed to account for the variability that occurs in geophysical measurements. Measurement variability can occur from many external stimuli. For example, as drilling proceeds in depth, natural physical variables, such as pressure and temperature, affect geophysical measurements because the phenomena which are measured by geophysical instrumentation are variable according to temperature and pressure. While temperature and pressure are variables that are somewhat predictable, unpredictable variables also need a failsafe mechanism to account for them. For example, the influx of fine particles into drilling fluid, altering its density is not a condition that can be assumed to happen, nor can the duration or magnitude of its effect be confidently quantified. Regardless, the effect of such a mechanism would have profound effects on the performance of the drilling fluid for its intended purpose. One technique to account for both random and predicted variability in the wellbore environment is the employment of a moving average technique. Moving averages weight data according to a discrete number of observations that is based on field-specific data, which can take the form of pre-drilling preparation (e.g. seismic interpretation) or the driller's experience. The discrete number of observations is known as the window or period. The window may be any length. The type of mathematical operation used in a moving average can also vary. One of the primary functions of moving averages is to dampen high amplitude but low frequency events. One of the critical factors in selecting a period is to provide an adequate amount of weighting to the most recent observations, while not suppressing variability in the data which could be indicative of a kick signal. Figure 5 provides an example of the effects of window size on the moving average reference in comparison to raw data. The plots demonstrate that as window size increases, the moving average plot shows an increasing amount of departure from the raw data. Spikes present in the raw data become more suppressed and the overall variation in the line produced by the moving average is also more suppressed.

Formation fluid influxes can occur as slow, gradual formation fluid leaks into the borehole annulus, but they can also occur as abrupt discharges. However, the rate of formation fluid influx is dynamic. Critical drilling fluid properties will change (e.g. density/viscosity) because of mixing with formation fluids. In particular, the drilling fluid density reduction will accelerate the formation fluid influx rate, as the confining pressure against the formation fluid pressure, which is maintained by the drilling fluid column in the wellbore, will decrease. The distinction among kicks is primarily dependent on the pressure gradient between the formation and the column of drilling fluid in the annulus. The kick detection capabilities of this process must be optimized for signal type, sampling rate, expected change in signal, and previous knowledge about the area being drilled. One contributing factor for achieving optimization is using multiple moving averages of varying window lengths.

Equation 5: Moving Average Difference Equation

$$y(n) = \frac{1}{Window\ Size}(x(n) + x(n-1) + \cdots + x\big(n - (Window\ Size - 1)\big))$$

Which is calculated using the MATLAB *filter* function. As window size increases, moving average plot become smoothed and the peaks become broader, relative to the raw data.

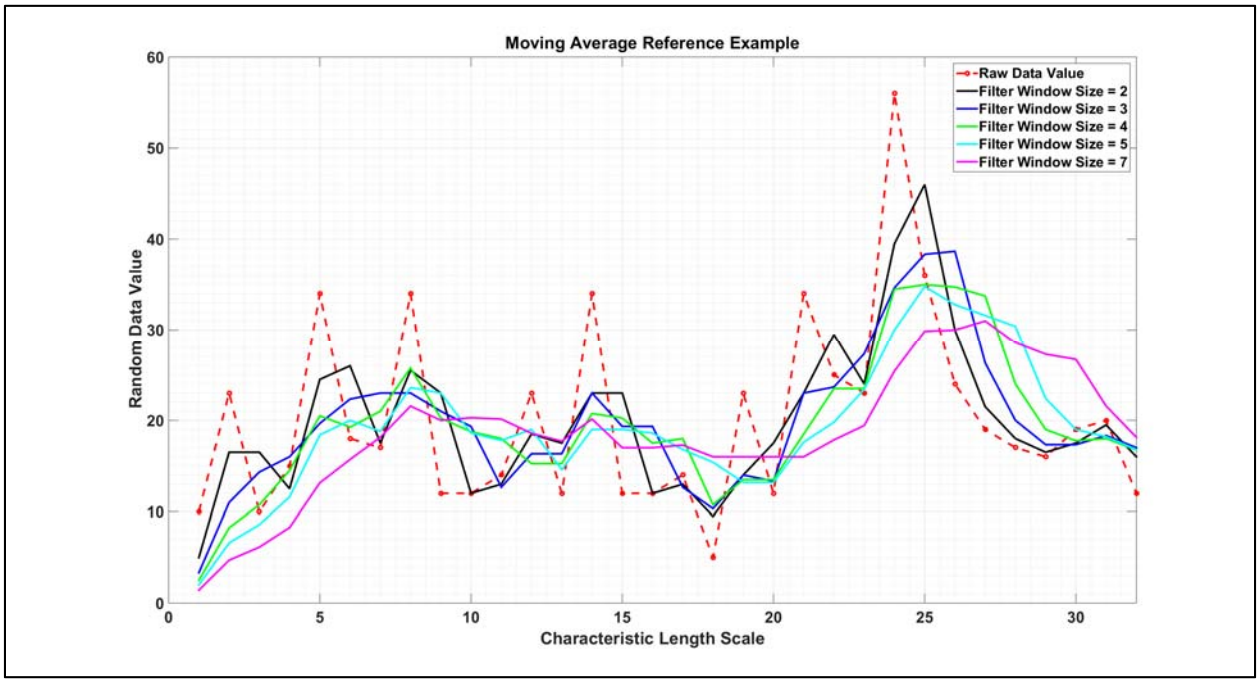

Figure 5: Moving average example.

A collection of sample plots exhibiting the effect of varying window size on a moving average is shown in Figure 5. This figure shows the raw data and moving average curves for various window sizes derived using the moving average difference equation. As the window size increases, the data become more smoothed. The amplitudes of the data become less prominent, with only the greatest amplitude events retaining their character.

A moving average using an arithmetic mean may not be sufficient by itself for identifying kicks. However, properties of the moving average line such as the instantaneous rate-of-change or the presence of an inflection point may be determined using mathematical operations to identify kicks in the raw data. One example of such mathematical operations is determining the instantaneous rate-of-change, or derivative, of the moving average line, as shown in Figure 6. Because the moving average line is calculated using a computer function, it does not lend itself easily to curve-fitting, making it difficult to determine the equation of the line.

One method to determine the numerical derivative of the moving average is to use the following approach:

Equation 6: Numerical Derivative Difference Equation

$$\Delta Y = [X(2) - X(1) \quad X(3) - X(2) \dots X(m) - X(m-1)]$$

Which calculates the difference between adjoining data points. These values are calculated using the MATLAB function *diff*. An approximate, numerical derivative may then be calculated if the results of the calculation using Equation 6 are then divided by a user-determined step size, ΔX, to calculate the numerical derivative (Equation 7).

In equation form:

Equation 7: Numerical Derivative Equation

$$\frac{dY}{dX} \cong \frac{\Delta Y}{\Delta X}$$

If the step size is sufficiently small (e.g. $\Delta X \leq 0.001$), this process provides a numerical derivative that is virtually equal to the analytically-determined derivative.

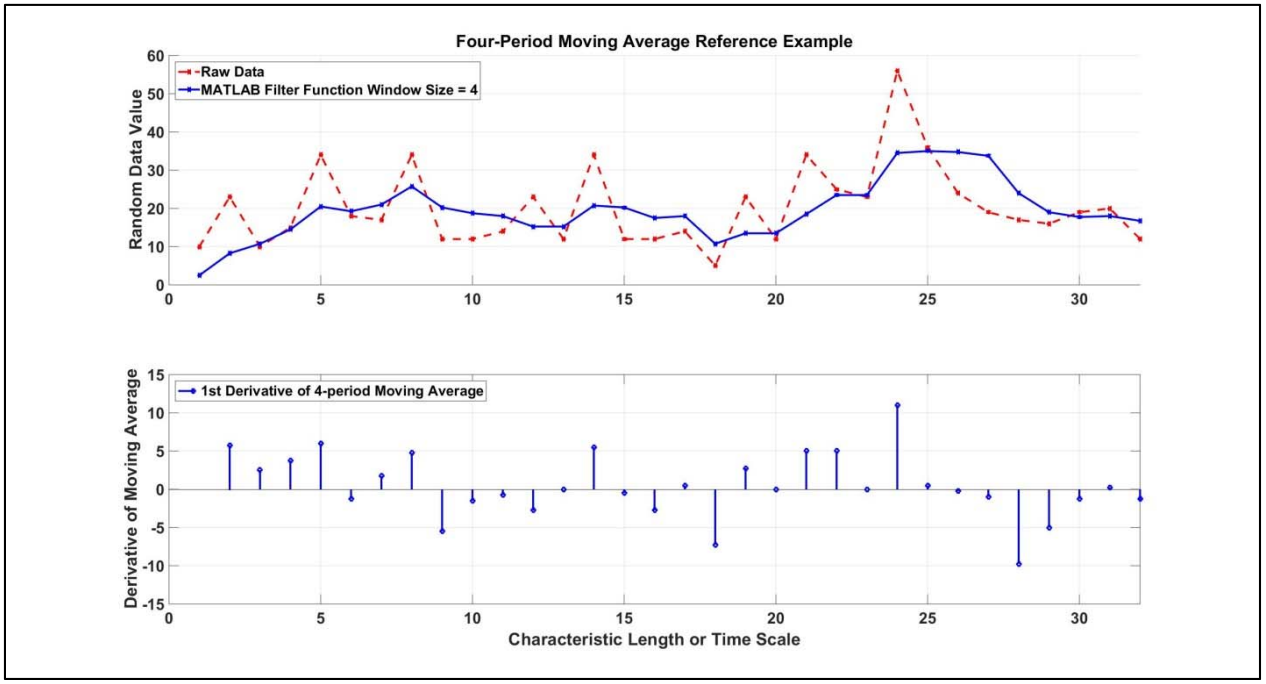

Figure 6: Moving average differential for kick identification.

A comparison of a window-size-four moving average and the first derivative of the window-size-four moving average is shown in Figure 6. The upper plot shows plots of the raw data (red) and a window-size-four moving average (blue). The moving average's smoothing tendency is demonstrated by the reduction of spikes when compared to the raw data. Local trends in the

dataset are preserved as demonstrated by the generally parallel behavior between the raw data and the moving average. Mathematical operations may be applied to a moving average to indicate regions of the dataset which may be indicative of a kick. In the lower plot, the derivative of the window-size-four moving average is stem-plotted (blue). The moving average derivative was determined numerically using the MATLAB "diff" function. The derivatives are plotted as stems to show the discrete behavior change from point-to-point. The magnitudes of the rates-of-change of the raw data are captured by the derivative and are demonstrated in the plot.

Identifying what part of a signal represents formation fluid influx into the wellbore is the first step in the kick detection approach. This involves detecting changes in dynamic properties of the signal options for analysis include statistical process control using a control chart and digital signal processing whereby segmentation of signals through DWT is used to identify signal energy characteristics; and also establishing links between segmented signals and physical properties/conditions in the borehole. Segmented units using DWT allow for an analysis of a localized area of a larger signal.

Template matching is also a viable method for kick detection. Here, a known template signal is compared against a larger portion of (often continuous source) data, and signal correlations values are output. The goal is to identify signals that match well with the criteria that are determined to be likely representative of a kick. For kick detection, a template is generated after collection and careful study of formation fluid influx scenarios in well logs.

After identification/recognition of kick-representative signal, the next step include: real-time monitoring which may involve the use of statistical parameters to model changing behavior using moving average methods; updating gains (increasing fluid influx) with adaptive algorithms to track quick variation of parameters; model-based monitoring using a database of models and applicable rules to correlate signals with kick/fluid type.

The control chart from ring resistivity data is designed taking into consideration the properties of the formation drilled through, drilling mud type, etc. It is used as a yardstick to determine if well log values are within acceptable "well-control" limits; and the variations are from expected sources such as formation change, change in drilling parameters, etc. Data from the first few hours of drilling are used to predict expected log readings with respect to formation change. Whenever the log readings fall outside the expected range, the control chart will provide indications of risk such as low, moderate, or high-risk level. By comparing real-time measurements to the expected values, the drilling process can be monitored to determine when well control issues arise.

Discretizing the waveform allows us to identify key features in the data. The positive and negative peaks in the data could represent one of many changes in the drilling process such as change in formation type, fluid loss, or fluid invasion.

In order to correctly determine a kick, a kick transient is identified and auto-correlated with the well log to identify the depth at which the kick is taking place.

2.4 PROOF-OF-CONCEPT MODELING

2.4.1 Rationale

One of the cornerstones of a viable kick detection system is the system's ability to provide as much advance warning as possible to the well operator that a kick has potentially occurred and is approaching the surface. The more time that is afforded the well operator to prepare for the approaching kick, the less time the kick is occurring, the less fluid the driller has to deal with in the annulus, and the safer the overall drilling process becomes.

Traditional kick detection methods involve examination of drilling fluid volume changes in either the annulus or the mud pit. Because the time delay between the kick fluid entry into the annulus and the onset of discernible signs of a kick to rig personnel, significant nonproductive time will be needed to suppress the kick.

The primary way that a kick detection system provides advance warning on a kick is to maximize the difference between the bit-to-rig floor travel times for the detection signal and kick, respectively. For maximization of advance warning (in equation form):

$$\varsigma - v_k \gg 0$$

Where, ς is the signal transmission rate (bits/time) and v_k is the kick velocity (length/time). The detection signal's bit-to-rig floor travel time varies according to the telemetry used for a given well. Mud-pulse telemetry utilizes pressure signals that are transmitted to the surface through the drilling fluid in the drillstring. The mud-pulse telemetry bit-to-surface travel time is the speed of sound through the drilling fluid, ranging from approximately 4,000 to 5,000 ft/s (1,200 to 1,500 m/s) (Arps, 1964). Thus, even for deepwater wells exceeding 5,000 ft (1,500 m), the mud-pulse telemetry bit-to-rig floor travel time is a matter of seconds.

Electromagnetic (EM) telemetry and hardwired telemetry are electronic signal transmission techniques used in MWD/LWD. EM telemetry transmits information by either inducing a magnetic field around the drillpipe and into the Earth, or generating an electric current into the drillpipe that returns through the Earth (Fertl et al., 1994). Hardwired telemetry uses electrical cables connecting the tool to the surface to transmit data (Fertl et al., 1994). Both EM and hardwired telemetries utilize electrical signals, which are significantly faster than the pressure wave velocity through the drilling fluid, resulting in virtually instantaneous data transmission to the surface.

2.4.2 Theoretical Gas Kick Travel Time

A gas kick occurs when formation gas enters the well annulus due to the formation pressure overcoming the drilling fluid pressure. Depending on the composition of the formation gas entering the annulus (e.g. methane, carbon dioxide, hydrogen sulfide) and the drilling fluid (e.g. oil-based vs. water-based), formation gases may either dissolve into the drilling fluid or form a discrete, separate phase in the well annulus (i.e. two-phase flow or bubbles). When bubbles form in the well annulus, they travel to the surface at a velocity which is the sum of the drilling fluid velocity and the gas-slip velocity (Zuber and Findlay, 1965). The gas-slip velocity is the velocity that the bubbles in two-phase flow travel relative to the drilling fluid. In equation form:

Equation 8: Kick Velocity

$$v_g = C_o v_m + v_s$$

Where, v_g is the gas velocity, C_o is the distribution factor, v_m is the drilling fluid annular velocity, and v_s is the gas-slip velocity. C_o is a function of bubble distribution relative to the cross-sectional region of maximum fluid flow, and can range from 1.0 to 1.5 (Hasan and Kabir, 1992; Zuber and Findlay, 1965). Gas-slip velocities vary according to drilling fluids, and are greater in viscous fluids than water (Johnson, 1991). A summary of gas kick simulations using experimental wells is found in Table 12.

Table 12: Simulated Gas Kick Data

Well Depth (m)	Kick Gas(es)	Drilling Fluid(s)	Time for Kick to Reach Surface (Pit Gain) (seconds)[minutes]	Gas-slip Velocity (m/s)[ft/s]
1,830[1*]	Nitrogen	Mud (8.6 lbs/gal)	1250 [~21]	0.4 [1.4]
15[2]	Air	Water	700 [~12]	0.25 to 0.55 [0.8 to 1.8]
15[2]	Air	Simulated mud (Xanthan gum)	400 [~7]	0.55 [1.8]
1,240[3*]	Air	Mud (9.1 lbs/gal)	Bimodal. Significant pit gain first observed at ~800 [~13], with the first peak occurring at ~1,200 [20]. Larger second peak observed at ~2,400 [40]	N/A
2,020[4*]	Argon and Nitrogen	Water-based mud (WBM): 1,030 kg/m^3 (8.6 lbs/gal) Oil-based muds (OBM): 1,300 kg/m^3 (10.8 lbs/gal) and 1,700 kg/m^3 (14.2 lbs/gal)	N/A	0.27 [0.9] for high-concentration gas kicks in both WBM and OBM 0.19 [0.6] for low to medium-concentration gas kicks in OBM

[1]Rader et al. (1975), [2]Johnson (1991), [3]Avelar et al. (2009), [4]Hovland and Rommetveit (1992)

[*] = Data from a real well

A field test in a 6,000 ft (1,830 m) well using nitrogen as the kick gas and an 8.6 pound-per-gallon (lbs/gal) drilling fluid produced a gas-slip velocity of 1.4 ft/s (0.4 m/s) (Rader et al., 1975). During this test, the test gas was first observed to reach the surface after 1,250 s (~21 min) (Rader et al., 1975). Kick simulations in a 39-ft (12-m) well using a kick gas:drilling fluid combination of air:mud produced an initial surficial gas outflow after approximately 400 s (~6.7 min) (Johnson, 1991). The same test apparatus using a combination of air:water produced an initial surficial gas outflow after approximately 700 min (~11.7 min) (Johnson, 1991). A field test in a 1,240-m test well using air as the kick gas and a 9.1 lbs/gal drilling fluid resulted in a bimodal surficial gas outflow, with significant surficial outflow after ~800 s (~13 min), an initial peak at ~1,200 s (~20 min), and a second, larger peak outflow at ~2,400 s (~40 min) (Avelar et al., 2009). From the experimental data found in Table 12, it is clear that the pit gain arrival time is a function of multiple, independent factors, such as kick gas and drilling fluid compositions and well depth.

Nevertheless, there is an established time delay between the kick gas influx and the kick gas arrival at the surface, even for very shallow wells. This time delay is on the order of several minutes and suggests that even mud-pulse telemetry, the slowest of the telemetry methods mentioned here, should provide minutes of advance warning of an approaching kick to the well operator.

2.4.3 Hypothetical Gas Kick Scenario Modeling

To illustrate the viability of this approach, a simulated model scenario was developed for a gas kick occurring in a well. Literature was reviewed on drilling fluid annular velocities, gas-slip velocities, signal size and processing times, and data telemetry rates. These data were then synthesized into a scenario that was considered to be typical for oil and gas exploration wells. A detection time was estimated for this method and a kick travel time from the well bottom to the surface. A graphical representation of a formation fluid influx scenario is shown in Figure 7. The modeling results for this scenario are found in Figure 8. The hypothetical gas kick modeling scenario parameters are found in Table 13.

Table 13: Hypothetical Gas Kick Scenario Parameters

Model Parameter	Parameter Value
Kick Occurrence Depth (D_K) (ft)	10,000
Speed-of-Sound in Drilling Fluid (ft/s)	5,000
Data Telemetry Rate (bits/s)	6
Geophysical Measurement Signal Size (bits)	16
Number of Geophysical Measurements Taken per Sampling Event, n	3
Geophysical Measurement Sampling Rate (k_s) (samples/depth interval)	2
Drilling Rate-of-Penetration (ROP) (depth interval/min)	1
Time Delay Between Sampling Events (s)	60
Number of Outlying Samples Needed for Kick ID	2
Rig Floor Data Processing Time (s)	5 (assumed)
Drilling Fluid Annular Velocity (ft/s)	1 to 4
Gas-Slip Velocity (V_{GS}) (ft/s)	1 to 4
Kick Velocity (V_K) (ft/s)	10

For the kick travel time modeling, a scenario was considered where a petroleum exploration well was being drilled.

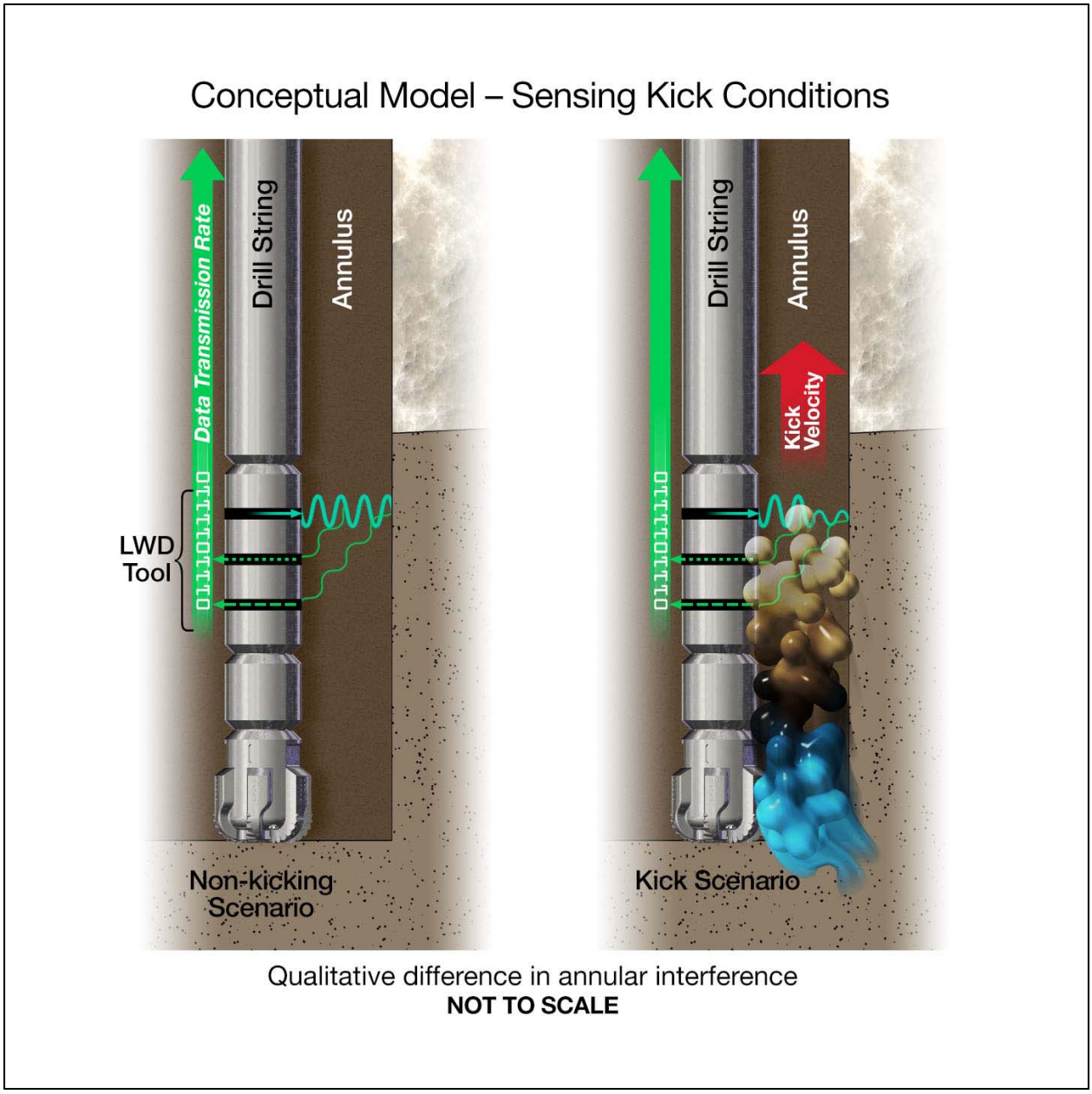

Figure 7: Kick detection conceptual model.

The drill intersects a geologic formation that produces a gas kick into the well at a depth of 10,000 ft. It was assumed that the well is vertical, and without deviations of any kind. A kick velocity was calculated as the sum of the drilling fluid annular velocity and the gas-slip velocity. Drilling fluid annular velocity is the quotient of the volumetric drilling fluid flow and the cross-sectional annular area through which the drilling fluid flows. Typical drilling fluid annular velocities range from approximately 1 ft/s to 10 ft/s, although the typical range is limited to 1 to 4 ft/s (Hall et al., 1950; Williams Jr. et al., 1951; Hopkin, 1967). Gas-slip velocity is the velocity at which gas bubbles rise relative to the fluid in which they are confined. Typical gas-slip velocities range from approximately 1 to 4 ft/s (Rader et al., 1975; Johnson et al., 1991; Hovland and Rommetveit, 1992; Avelar et al., 2009). The bubble distribution coefficient, C_o, ranges from 1.0 to 1.5. To provide a worst-case scenario for kick travel time based on these value ranges, a

constant kick velocity of 10 ft/s was assumed. This value arose from a drilling fluid annular velocity of 4 ft/s, a bubble distribution coefficient of 1.5, and gas-slip velocity of 4 ft/s. In equation form:

$$v_k = 1.5 * (4\ feet/second) + 4\ feet/second = 10\ feet/second$$

Using the assumed kick velocity,$\boldsymbol{V_K}$, the kick travel time is calculated as a function of the depth of kick occurrence, $\boldsymbol{D_K}$. In equation form:

Kick Travel Time Calculation

$$\boldsymbol{Kick\ Travel\ Time} = \frac{\boldsymbol{D_K}}{\boldsymbol{V_K}}$$

This relationship is the red plot in Figure 8.

The Method Detection Time was then calculated, which is the time needed for this method to sense a kick occurring in the borehole, compress and transmit data to the surface, process the data at the surface, and transmit a warning to the well operator.

Method Detection Time Calculation

$$\boldsymbol{Method\ Detection\ Time} = \boldsymbol{Data\ Collection\ Time} + \boldsymbol{Data\ Transmission\ Time} + \boldsymbol{Data\ Processing\ Time}$$

In the Data Collection Time calculation, which is defined as the time needed to sense a kick in the borehole, a geophysical measurement sampling rate, $\boldsymbol{k_s}$, was considered for a petroleum exploration well to be two samples per depth interval. Using a typical drilling rate-of-penetration for petroleum exploration wells, **ROP**, a sampling rate was calculated. Two consecutive outlying samples were assumed to be needed to positively determine that a kick has occurred. Then the Data Collection Time was calculated as the quotient of the number of samples needed to make a positive kick determination, **n**, and the data sampling rate.

Data Collection Time Calculation

$$\boldsymbol{Data\ Collection\ Time} = \frac{\boldsymbol{n}}{(\boldsymbol{ROP} * \boldsymbol{k_s})}$$

In the calculation of the time needed to transmit the required amount of data from the well bottom to the surface, the number of sampling events, the number of geophysical measurements per sampling event, and the amount of memory used per geophysical measurement were

considered. The product of these parameters represents the amount of memory needed to accurately define the kick occurring in the borehole. A typical data transmission rate was then considered, assuming mud-pulse telemetry as the telemetry method. Literature values for mud-pulse telemetry range from 3 to 5 bps for pressure wave mud-pulse telemetry methods to 6 to 24 bps for mud siren telemetry methods. This scenario assumed the use of mud siren telemetry and a telemetry rate of 6 bps. The Data Transmission Time was then calculated as the quotient of the necessary amount of memory and the data telemetry rate.

Data Transmission Time Calculation

$$\textbf{\textit{Data Transmission Time}} = \frac{(\textbf{\textit{Number of Sampling Events}} * \frac{\textbf{\textit{Geophysical Measurements}}}{\textbf{\textit{Sampling Event}}} * \frac{\textbf{\textit{Memory Size}}}{\textbf{\textit{Geophysical Measurement}}})}{\textbf{\textit{Data Telemetry Rate}}}$$

The amount of time needed to process the data at the surface, make the comparison to determine if a kick has occurred, and generate and transmit a warning signal to the operator was then considered. This process was treated as limited by computer processor speed, which is a relatively fast process. A value of 5 s was assumed for Data Processing Time at the surface.

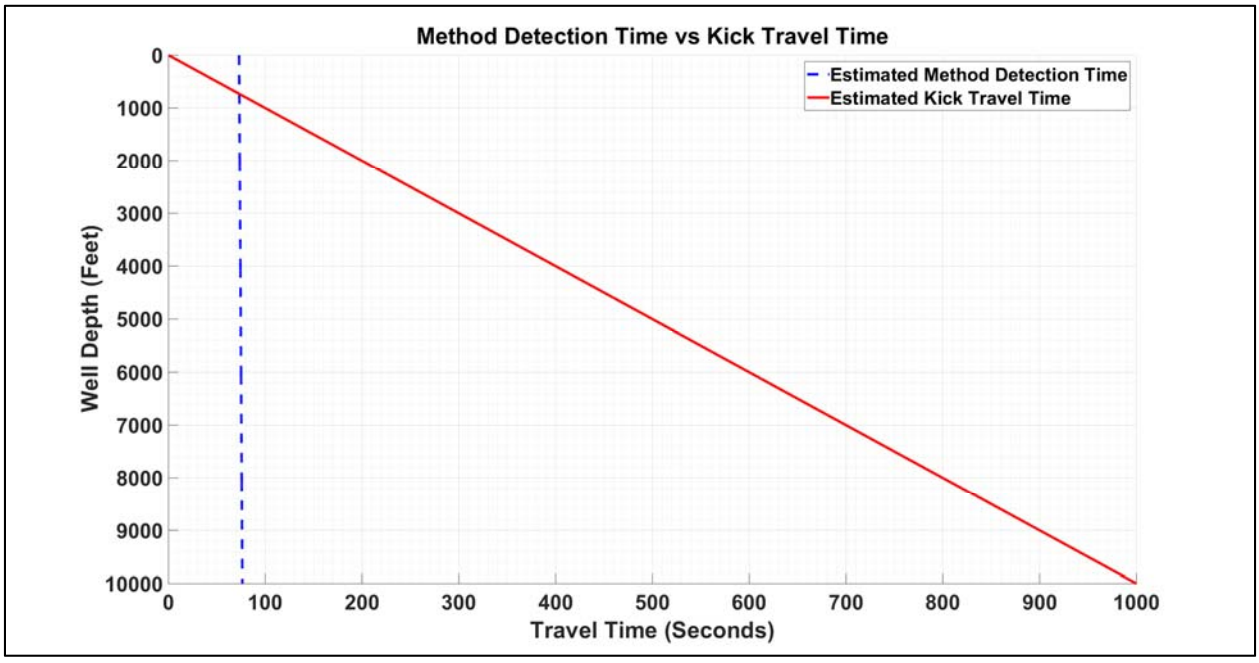

Figure 8: Modeling results for the gas kick scenario.

A plot comparing the estimated time for a gas kick to travel from the well bottom to the surface to the estimated time required for the kick detection technique described in this document to alert

the well operator that a potential kick has occurred as a function of well depth. Initially, kick travel time is faster than kick detection time because of the data transmission limitations inherent in mud-pulse telemetry. For the given set of parameters, the break-even depth is approximately 800 ft. Beyond this depth, the kick detection time is faster than kick travel time. For the depth of typical exploration wells, which is approximately 6,000–7,000 ft, the time advantage presented by the kick detection method is significant.

For the given parameters, the Estimated Method Detection Time is approximately 75 s, and the Estimated Kick Travel Time is approximately 1,000 s. The difference between these values represents a significant time advantage for the well operator to take steps to avert any further loss of well control.

3. FUTURE WORK

Future work is ongoing and is scheduled to include computational modeling, lab/experimental work for calibrating instrument responses to fluid mixtures, and use of field data from wells that are known to have experienced a loss of control event for technique validation. The data from these activities will be used to further develop the method described in this report, such as determining which statistical treatments are the most appropriate kick indicator.

Future field data experiments will involve using geophysical well logs from wells that have experienced documented loss-of-control events to test and validate the approach described in this document. Tests such as these would act as a simulation for use in a real drilling scenario.

Process validation will occur by using field data or by laboratory experimentation. Field data would be acquired by partnering with a private oil company. The partnership would likely result in the exchange of unprocessed field data from geophysical instrumentation for exclusive licensure of the technology once the process is validated. Licensure to private companies is dependent on the other step in the immediate future of this project, which is acquisition of a U.S. patent. A U.S. patent is essential for permitting licensure of the technology described in this document for use and sale by private companies.

3.1 FORMATION FLUID EFFECTS ON DRILLING FLUID PROPERTIES - "KICK FINGERPRINTING"

"Kick fingerprinting" is the concept of identifying a kick fluid's composition by using the unique combination of geophysical well log responses that result because of a physical property change in the drilling fluid in the wellbore because of formation fluid mixing. The formation fluid mixing with drilling fluid results in a composite fluid whose physical properties are distinctly different from both the pure drilling fluid and the pure kick fluid. It is possible to quantify physical property variations with certain volume fractions of certain formation fluids mixed with drilling fluid in the annulus. Thus, it is possible to ascertain the identity and the amount of a certain formation fluid based on the collective instrument responses.

Experiments to Refine Kick Fingerprinting

Future laboratory experiments to refine kick fingerprinting include mixing simulated formation fluids (e.g. air, brine, and freshwater) with drilling fluids at controlled temperatures, pressures, and volume fractions in order to determine the mixing laws that govern composite mixture physical properties.

Laboratory experimentation would involve designing and executing experiments using the Multi-Sensor Core Logger (MSCL) at the NETL Morgantown. The experiments would be designed to simulate a borehole into which gas and liquid kicks invaded, and measuring the physical property changes that occur after the kick invasion. The MSCL has physical instrumentation that measures gamma density, compressional (*p*-wave) velocity, and non-contact electrical resistivity, which are the primary geophysical parameters prescribed by the kick detection method described in this document. Data from such experiments would assist in determining which mixing laws control composite fluid properties, and if specific mixing law parameters (e.g. exponents and/or coefficients) exist for specific composite fluid combinations (e.g. air mixed into a water-based drilling fluid).

4. CONCLUSIONS

This report presents a method for early, low-cost kick detection by using geophysical measurements from while-drilling instrumentation located near the bit. The method is based on the principle that physical properties of drilling fluids which are measured by geophysical instrumentation in the wellbore (e.g. bulk density, electrical resistivity/conductivity, and compressional velocity) are known by the driller. In a scenario where a kick occurs, a formation fluid enters the wellbore and mixes with the drilling fluid, resulting in a composite fluid whose physical properties are distinctly different from either the drilling fluid or the formation fluid. This physical property contrast is sensible by the geophysical instrumentation, which indicates that a formation fluid has invaded the wellbore. First principles and published literature support the assertion that geophysical instrumentation deployed in the wellbore as part of the while-drilling tool suites is able to sense the contrast. Hewitt (1978) describes methods for detecting two-phase flow in pipes using gamma density methods, electrical impedance methods, and acoustic velocity methods similar those used by geophysical instrumentation deployed in the borehole. Bryant (1991) and Patil (2010) also provide data showing detectable changes in electrical measurements after drilling fluids have been mixed with kick fluids.

Moving-average filtering in conjunction with numerical differentiation show promise as methods for smoothing noise in data to facilitate kick identification.

First-order calculations provided in this report suggest that the kick detection method can sense a kick in the wellbore, transmit the data to the surface, analyze the data, and generate a warning to the driller significantly faster than the kick fluid can travel. The resulting time advantage could provide the driller with sufficient time to take actions to suppress the kick event before its intensity grows.

Future work is planned to develop and refine methods to support kick fluid identification and volume fraction estimation, and develop models to describe kick fluid mass transfer in the annulus in time and space.

5. REFERENCES

Ali, T. H.; Haberer, S. M.; Says, I. P.; Ubaru, C. C.; Laing, M. L.; Helgesen, O.; Liang, M.; Bjelland, B. Automated Alarms for Smart Flowback Fingerprinting and Early Kick Detection. Presented at SPE/IADC Drilling Conference and Exhibition, Amsterdam, The Netherlands, Mar 5–7, 2013; IADC/SPE 163474.

Archie, G. E. The electrical resistivity log as an aid in determining some reservoir characteristics. *Pet Tech* **1942,** *5*.

Arps, J. J. The subsurface telemetry problem – A practical solution. *Journal of Petroleum Technology* **1964,** *16*, 487–493.

Avelar, C. S.; Ribeiro, P. R.; Sepehrnoori, K. Deepwater gas kick simulation. *Journal of Petroleum Science and Engineering* **2009,** *67*, 13–22.

Baker Hughes. *Smart Flowback Fingerprinting Service*; Baker Hughes: Houston, TX, 2014.

Batzle, M.; Wang, Z. Seismic properties of pore fluids. *Geophysics* **1992,** *57*, 1396–1408.

Bern, P. A.; Zamora, M.; Slater, K. S.; Hearn, P. J. The influence of drilling variables on barite sag. In *SPE Annual Technical Conference and Exhibition*. Society of Petroleum Engineers, Jan 1996.

Bourgoyne Jr., A. T.; Millheim, K. K.; Chenevert, M. E.; Young, Jr., F. S. *Applied Drilling Engineering*; SPE Textbook Series, 1986.

Bryant, T. M.; Grosso, D. S.; Wallace, S. N. Gas-Influx Detection with MWD Technology. *SPE Drilling Engineering* **1991,** *6*, 273–278.

Caenn, R.; Darley, H. C.; Gray, G. R. *Composition and properties of drilling and completion fluids*; Gulf Professional Publishing, 2011.

Carcione, J. M.; Poletto, F. Sound Velocity of Drilling Mud Saturated with Reservoir Gas. *Geophysics* **2000,** *65*, 646–651.

Choe, J.; Schubert, J. J.; Juvkam-Wold, H. C. Well control analyses on extended reach and multilateral trajectories. In *Offshore Technology Conference*; Offshore Technology Conference, Jan 2004

Crowo, A. Ultrasound measurements on oil-based drilling mud. *Flow Meas. Instrum.* **1990,** *1*, 113–117.

Ellis, D. V.; Singer, J. M. *Well Logging for Earth Scientists*; Springer, Dordrecht, 2007; pp 692.

England, W. A.; Mackenzie, A. S.; Mann, D. M.; Quigley, T. M. The movement and entrapment of petroleum fluids in the subsurface. *Journal of the Geological Society* **1987,** *144*, 327–347.

Fertl, W. H., Chapman, R. E., Hotz, R. F., Eds. *Studies in Abnormal Pressures, Developments in Petroleum Science*; Elsevier Science, Amsterdam, 1994; p 38.

Guo, X.; He, S.; Liu, K.; Song, G.; Wang, X.; Shi, Z. Oil generation as the dominant overpressure mechanism in the Cenozoic Dongying depression, Bohai Bay Basin, China. *AAPG bulletin* **2010,** *94*, 1859–1881.

Hall, H. N.; Thompson, H.; Nuss, F. Ability of drilling mud to lift bit cuttings. *J. Pet. Technol.* **1950,** *2*, 35–46.

Halliburton, Drillworks Geomechanics. https://www.landmark.solutions/Drillworks-Geomechanics (accessed May 10, 2016).

Hasan, A. R.; Kabir, C. S. Two-phase flow in vertical and inclined annuli. *International Journal of Multiphase Flow* **1992,** *18*, 279–293.

Hewitt, G. F. Measurement of two-phase flow parameters, **1978**. *Academic Press*.

Hopkin, E. A. Factors affecting cuttings removal during rotary drilling. *J. Pet. Technol.* **1967,** *19*, 807–814.

Hovland, F.; Rommetveit, R. Analysis of Gas-Rise Velocities from Full-Scale Kick Experiments. In SPE Annual Technical Conference and Exhibition, Society of Petroleum Engineers, 1992.

Jensen, R. H.; Kurata, F. Density of liquefied natural gas. *Journal of Petroleum Technology* **1969,** *21*, 683–691.

Johnson, A. B. Gas-rise velocities during kicks. *SPE Drilling Engineering* **1991,** *6*, 257–263.

Lamont, N. Relationships between the Mud Resistivity, Mud Filtrate Resistivity, and the Mud Cake Resistivity of Oil Emulsion Mud Systems. *J. Pet. Technol.* **1957,** *9*, 51–52.

Lee, A. L.; Gonzalez, M. H.; Eakin, B. E. The viscosity of natural gases. *Journal of Petroleum Technology* **1966,** *18*, 997–1000.

Nesbitt, B. E. Electrical resistivities of crustal fluids. *J. Geophys. Res. Solid Earth 1978–2012* **1993,** *98*, 4301–4310.

Osborne, M. J.; Swarbrick, R. E. Mechanisms for generating overpressure in sedimentary basins: a reevaluation. *AAPG bulletin*, **1997,** *81*, 1023–1041.

Overton, H. L.; Lipson, L. B. *A correlation of the electrical properties of drilling fluids with solids content*; Society of Petroleum Engineers, 1958; SPE-1171-G.

Patil, P. A.; Gorek, M.; Folberth, M.; Hartman, A.; Forgang, S.; Fulda, C.; Reinecke, K. M. Experimental Study of Electrical Properties of Oil-Based Mud in the Frequency Range from 1 to 100 MHz. *SPE Drilling and Completion* **2010,** *25*, 380.

Patnode, H. W. Relationship of drilling mud resistivity to mud filtrate resistivity. *J. Pet. Technol.* **1949,** *1*, 14–16.

Rader, D.W.; Bourgoyne, A.T.; Ward, R. H. Factors affecting bubble-rise velocity of gas kicks. *Journal of Petroleum Technology* **1975,** *27*, 571–584.

Saasen, A.; Jordal, O. H.; Burkhead, D.; Berg, P. C.; Løklingholm, G.; Pedersen, E. S.; Harris, M. J. Drilling HT/HP wells using a cesium formate based drilling fluid. In *IADC/SPE Drilling Conference*; Society of Petroleum Engineers, 2002.

Samouëlian, A.; Cousin, I.; Tabbagh, A.; Bruand, A.; Richard, G. Electrical resistivity survey in soil science: a review. *Soil and Tillage Research* **2005,** *83*, 173–193.

Schnoebelen, D. J.; Bugliosi, E. F.; Krothe, N. C. Delineation of a Saline Ground-Water Boundary from Borehole Geophysical Data. *Groundwater* **1995,** *33*, 965–976.

Speers, R. A.; Holme, K. R.; Tung, M. A.; Williamson, W. T. Drilling fluid shear stress overshoot behavior. *Rheol. Acta* **1987,** *26*, 447–452. DOI:10.1007/BF01333845.

Standing, M. B.; Katz, D. L. Density of crude oils saturated with natural gas. *Transactions of the AIME* **1942a,** *146*, 159–165.

Standing, M. B.; Katz, D. L. Density of natural gases. *Transactions of the AIME* **1942b,** *146*, 140–149.

Swarbrick, R. E. Reservoir diagenesis and hydrocarbon migration under hydrostatic palaeopressure conditions. *Clay Minerals*, **1994**, *29*, 473–474.

Thomas, L. K.; Hankinson, R. W.; Phillips, K. A. Determination of acoustic velocities for natural gas. *Journal of Petroleum Technology* **1970,** *22*, 889–895.

Tixier, M. P.; Alger, R. P.; Doh, C. A. *Sonic Logging. Petroleum Transactions*; SPE 1115-G. T. P. 8063; AIME, 1958; pp 106–114.

Ucok, H.; Ershaghi, I.; Olhoeft, G. R. Electrical resistivity of geothermal brines. *J. Pet. Technol.* **1980,** *32*, 717–727.

Urish, D. W. The Practical Application of Surface Electrical Resistivity to Detection of Ground-Water Pollution. *Groundwater* **1983,** *21*, 144–152.

van Ruth, P., Hillis, R.; Tingate, P. The origin of overpressure in the Carnarvon Basin, Western Australia: implications for pore pressure prediction. *Petroleum Geoscience*, **2004,** *10*, 247-257.

Wang, T.; Yu, L.; Fanini, O. Multicomponent induction response in a borehole environment. *Geophysics* **2003,** *68*, 1510–1518. DOI:10.1190/1.1620624.

Wang, Z.; Nur, A. M.; Batzle, M. L. Acoustic velocities in petroleum oils. *J Pet Tech* **1990,** *42*, 192–200.

Williams Jr, C. E.; Bruce, G. H. Carrying capacity of drilling muds. *J. Pet. Technol.* **1951,** *3*, 111–120.

Zuber, N.; Findlay, J. A. Average volumetric concentration in two-phase flow systems. *Journal of Heat Transfer* **1965,** *87*, 463–468.

Sean Plasynski
Executive Director
Technology Development & Integration Center
National Energy Technology Laboratory
U.S. Department of Energy

John Wimer
Associate Director
Strategic Planning
Science & Technology Strategic Plans & Programs
National Energy Technology Laboratory
U.S. Department of Energy

Roy Long
Technology Manager
Science & Technology Strategic Plans & Programs
National Energy Technology Laboratory
U.S. Department of Energy

Elena Melchert
Director
Division of Upstream Oil and Gas Research
U.S. Department of Energy

Cynthia Powell
Executive Director
Research & Innovation Center
National Energy Technology Laboratory
U.S. Department of Energy